Supplementary Information (SI)

Design, Synthesis, Biological Evaluation and Molecular Docking Studies of Quinoline-Anthranilic Acid Hybrids as Potent Anti-Inflammatory Drugs

Sidra Siddique,[1] Khalid Hussain,[1,2]* Naureen Shehzadi,[1] Muhammad Arshad,[3]* Muhammad Nadeem Arshad,[4] Sadaf Iftikhar,[5] Farhat Saghir,[1,2] Ayisha Shaukat,[1] Muhammad Sarfraz,[3] Nisar Ahmed[6]*

[1]Punjab University College of Pharmacy, University of the Punjab, Allama Iqbal Campus, Lahore, Pakistan.

[2]Faculty of Pharmacy, The University of Lahore, Lahore, Pakistan.

[3]Institute of Chemistry, The Islamia University of Bahawalpur, Bahawalpur- 63100, Pakistan.

[4]Chemistry Department, Faculty of Science, and Center of Excellence for Advanced Material Research, King Abdulaziz University, Jeddah 21589, P.O. Box 80203, Saudi Arabia.

[5]Department of Pharmacy, University of South Asia, Lahore, Pakistan

[6]School of Chemistry, Cardiff University, Main Building, Park Place, Cardiff, CF10 3AT, UK.

***Corresponding Author's Email:**
khalid.hussain@pharm.uol.edu.pk (K.H.)
muhammad.arshad@iub.edu.pk (M.A.)
AhmedN14@cardiff.ac.uk (N.A.)

Table of Contents

1 Materials and General Methods 3

1.1. Glassware, Solvents and Reagents 3

1.2. Chromatography and Instrumentation 3

1.3. Naming of Compounds 4

2 Druglikeness studies 4

3 Molecular docking studies 6

4 Experimental Data 15

4.1 Synthesis of Compounds 15

4.1.1 Synthesis of acetamides (L/T/A)[1] 15

4.1.2 Synthesis of 1(a-c)[3] 15

5 Spectroscopic Data 17

5.1 ^{1}H NMR ($CDCl_3$, 600 MHz) of 2-Chloroquinoline-3-carbaldehyde (1a) 17

5.2 ^{13}C NMR ($CDCl_3$, 150 MHz) of 2-Chloroquinoline-3-carbaldehyde (1a) 18

5.3 DEPT-135 NMR ($CDCl_3$, 150 MHz) of 2-Chloroquinoline-3-carbaldehyde (1a) 19

5.4 ^{1}H NMR ($CDCl_3$, 600 MHz) of 2-Chloro-6-methylquinoline-3-carbaldehyde 1b 20

5.5 ^{13}C NMR ($CDCl_3$, 150 MHz) of 2-Chloro-6-methylquinoline-3-carbaldehyde 1b 21

5.6 DEPT-135 NMR ($CDCl_3$, 150 MHz) of 2-Chloro-6-methylquinoline-3-carbaldehyde 1b 22

5.7 ^{1}H NMR ($CDCl_3$, 600 MHz) of (2-Chloroquinolin-3-yl)methanol (2a) 22

5.8 ^{13}C NMR ($CDCl_3$, 150 MHz) of (2-Chloroquinolin-3-yl)methanol (2a) 24

5.9 DEPT-135 NMR ($CDCl_3$, 150 MHz) of (2-Chloroquinolin-3-yl)methanol (2a) 25

5.10 ^{1}H NMR (DMSO, 600 MHz) of (2-Chloro-6-methylquinolin-3-yl)methanol) (2b) 26

5.11 ^{13}C NMR (DMSO, 150 MHz) of (2-Chloro-6-methylquinolin-3-yl)methanol) (2b) 27

5.12 DEPT-135 NMR (DMSO, 150 MHz) of (2-Chloro-6-methylquinolin-3-yl)methanol) (2b) 29

5.13 ^{1}H NMR ($CDCl_3$, 400 MHz) of (2-Chloroquinolin-3-yl)methyl 2-aminobenzoate (5a) 30

5.14 ^{13}C NMR ($CDCl_3$, 400 MHz) of (2-chloroquinolin-3-yl)methyl-2-aminobenzoate (5a)31

5.15 ^{1}H NMR ($CDCl_3$, 400 MHz) of (2-Chloro-6-methylquinolin-3-yl)methyl 2-aminobenzoate (5b) 32

5.16 ^{13}C NMR ($CDCl_3$, 100 MHz) of (2-Chloro-6-methylquinolin-3-yl)methyl 2-aminobenzoate (5b) 33

5.17 ^{1}H NMR (300 MHz, DMSO) of (2-Chloro-6-methoxyquinolin-3-yl)methyl-2-aminobenzoate (5c) 34

5.18 ^{13}C NMR (75 MHz, DMSO) of (2-chloro-6-methoxyquinolin-3-yl)methyl-2-aminobenzoate (5c) 36

6 X-Ray Crystallography Data (XRD) 37

7 References 38

1 Materials and General Methods

1.1. Glassware, Solvents and Reagents

All manipulations were performed with oven-dried (110 °C for a minimum of 12 h) dried glassware. All solvents were commercially supplied or distilled before use (MeOH, DMF, MeCN, CH_2Cl_2). Reagents were purchased from commercial sources and used as received.

1.2. Chromatography and Instrumentation

Thin layer chromatography (TLC) was performed using Merck Kieselgel 60 F254 fluorescent treated silica, which was visualized under UV light, or by staining with aqueous basic potassium permanganate ($KMnO_4$) followed by heating.

Flash column chromatography (FCC) was carried out using Merk silica gel (60 Å, 230–400 mesh, 40–63 μm) using a suitable mobile phase as stated.

NMR spectra were recorded at various field strengths, as indicated, using Bruker 300 MHz, 400 MHz, and 600 MHz for ^{1}H and ^{13}C acquisitions. All NMR spectra were recorded at 25 °C unless otherwise stated. Chemical shifts (δ) are reported in parts per million (ppm) and referenced $CDCl_3$ (^{1}H: 7.26 ppm; ^{13}C: 77.10 ppm) or DMSO-d_6 (^{1}H: 2.50 ppm; ^{13}C: 39.52 ppm). Coupling constants

(*J*) are given in Hertz (Hz) and refer to apparent multiplicities (s = singlet, d = doublet, t = triplet, m = multiplet, br = broad signal, dd = doublet of doublets, etc.). The ^{1}H NMR spectra are reported as follows: chemical shift (multiplicity, coupling constants, number of protons). ^{13}C NMR values are reported up to one decimal after rounding off the second decimal digit.

X-ray Crystallography (XRD) was performed using Bruker D8 Venture with PHOTON II detector and Mo microfocus source (λ= 0.71073 Å) were used for the present study.

IR spectra were recorded neat (ATR sampling) on Agilent FT-IR spectrophotometer. Selected absorption maxima (ν_{max}) are reported in wavenumbers (cm^{-1}).

For In vitro **Bioactivities,** thermostatic water bath (M-270, Memmert, Germany), centrifuge machine (80-2 electronic centrifuge), pH meter (Schott gerate, Germany) double beam UV spectrophotometer (UV-2550, Shimadzu Corporation, Japan) were used.

1.3. Naming of Compounds

Compound names are those generated by ChemDraw Professional 20.0 software (PerkinElmer), following the IUPAC nomenclature.

2 Druglikeness studies

Table S1. Physicochemical, drug-likeness, pharmacokinetic, and toxicity predictions of compound **5a-c**

Parameter	**Compound 5a**	**Compound 5b**	**Compound 5c**	**Software**
Physicochemical properties				
MW (Molecular weight) g/mol	312.75	326.78	342.78	swissADME
No. of heavy atoms	22	23	24	swissADME
No. of RB (rotatable bonds)	4	4	5	swissADME
No. of aromatic heavy atoms	16	16	16	swissADME
HBA (Hydrogen bond acceptors)	3	3	4	swissADME
Fraction Csp3	0.06	0.11	0.11	swissADME
TPSA (Å²)	65.21	65.21	74.44	swissADME
MR (Molar Refractivity)	86.92	91.89	93.42	swissADME
Consensus Log Po/w	3.45	3.82	3.5	swissADME
Pure water solubility (mg/L)	3.54	1.099	2.53	preADMET
Water solubility class	Moderate	Moderate	Moderate	swissADME

Buffer solubility (mg/L)	28.53	12.16	16.21	preADMET
Absorption				
HIA	96.48	96.54	96.64	preADMET
	High	High	High	swissADME
Caco2 (permeability in nm/sec)	21.31	21.62	21.37	preADMET
MDCK (permeability in nm/sec	7.38	0.32	1.11	preADMET
Skin Penetrability (log Kp	-5.11	-4.94	-5.31	swissADME
cm/sec)	-3.08	-3.01	-3.26	preADMET
Distribution				
BBB (blood brain barrier)	Yes	Yes	Yes	swissADME
	0.57	0.16	0.31	preADMET
PPB (Plasma Protein Binding)	89.83	88.24	87.30	preADMET
P-gp substrate	No	No	No	swissADME
P-gpinhibition	Inhibitor	Inhibitor	Inhibitor	preADMET
Metabolism				
CYP3A4 substrate	Weakly	Weakly	Weakly	preADMET
CYP2D6 substrate	None	None	None	preADMET
CYP2C19 inhibition	Yes	Yes	Yes	Both
CYP2C9 inhibition	Yes	Yes	Yes	Both
CYP2D6 inhibition	yes	Yes	yes	swissADME
	None	None	None	preADMET
CYP1A2 inhibitor	Yes	Yes	Yes	swissADME
CYP3A4 inhibition	Yes	Yes	Yes	Both

HIA: human intestinal absorption, **Caco2**: cells which originate from human colon adenocarcinoma, **MDCK**: madin−darby canine kidney, **p-gp**: p glycoprotein, an efflux protein

Table S2. Medicinal Chemistry, and toxicity of hybrids

Medicinal Chemistry				
PAINS	0 alert	0 alert	0 alert	swissADME
Brenk	2 alerts	2 alerts	2 alerts	swissADME
Leadlikeness	No	No	No	swissADME
Synthetic accessibility	2.25	2.37	2.35	swissADME
Toxicity				
AMES test	Mutagen	Mutagen	Mutagen	preADMET
Carcinogenicity (Mouse)	Negative	Negative	Negative	preADMET
Carcinogenicity (Rat)	Negative	Negative	Negative	preADMET
Inhibition of HERG	Medium risk	Medium risk	Medium risk	preADMET
TA100(10RLI)	Positive	Positive	Positive	preADMET
TA100(NA)	Negative	Negative	Positive	preADMET
TA1535(10RLI)	Negative	Negative	Negative	preADMET

TA1535(NA)	Negative	Negative	Negative	preADMET

3 Molecular docking studies

protein- native ligand complex (in pdb)

protein- native ligand complex (redocked)

A –UTJ (TNF-α)

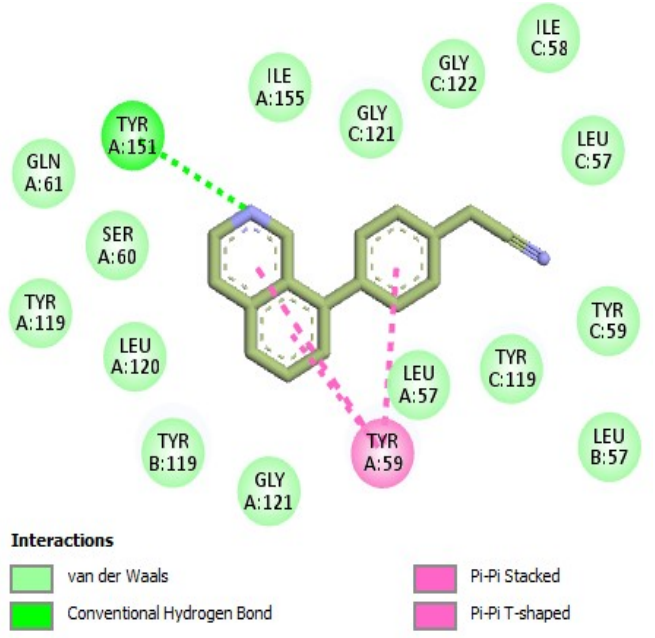

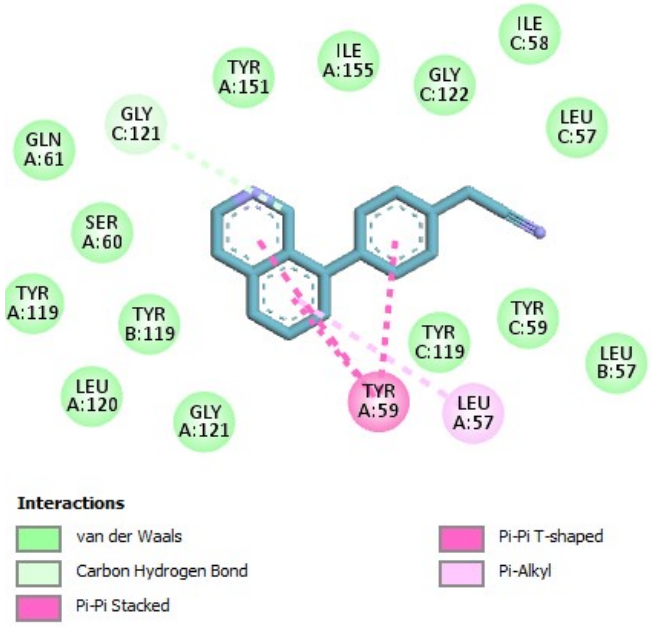

B -QY 1 (FLAP)

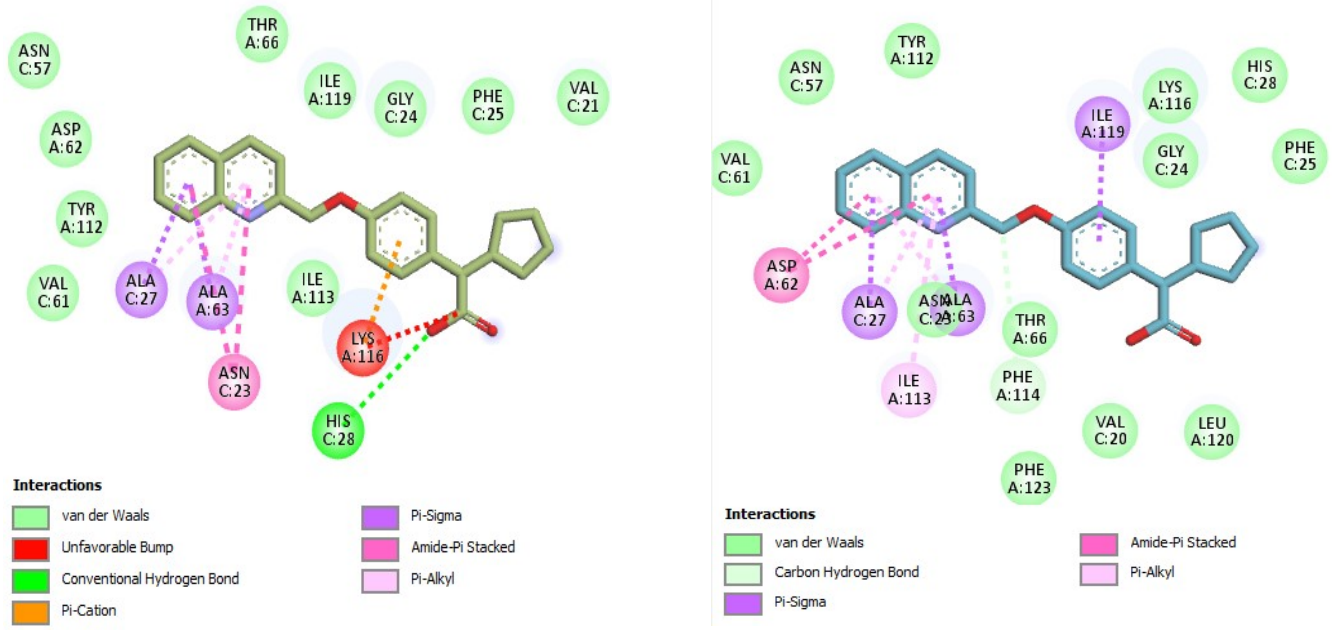

C –ACD (COX-II)

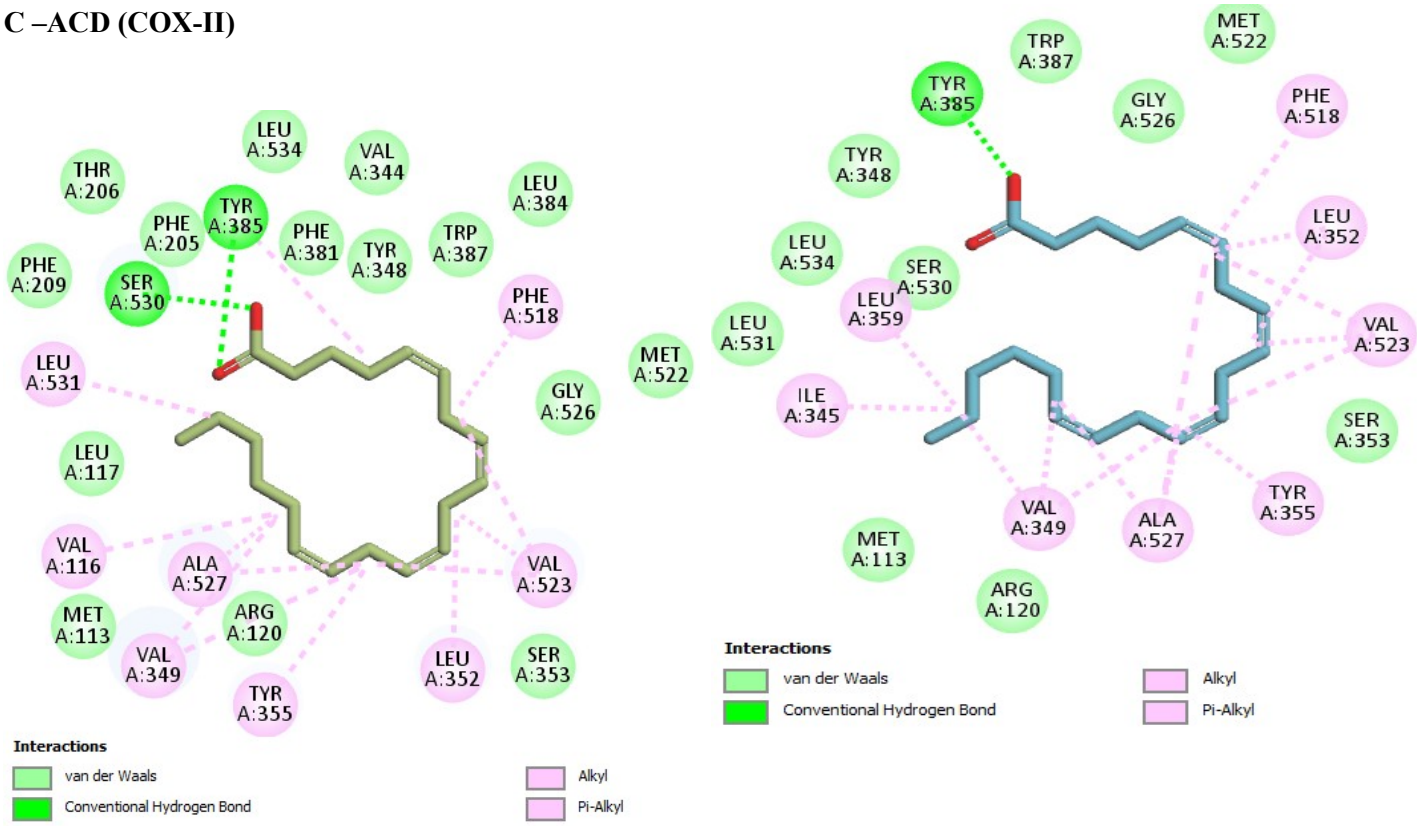

Figure.S1. comparison of native ligand with redocked native ligand

A

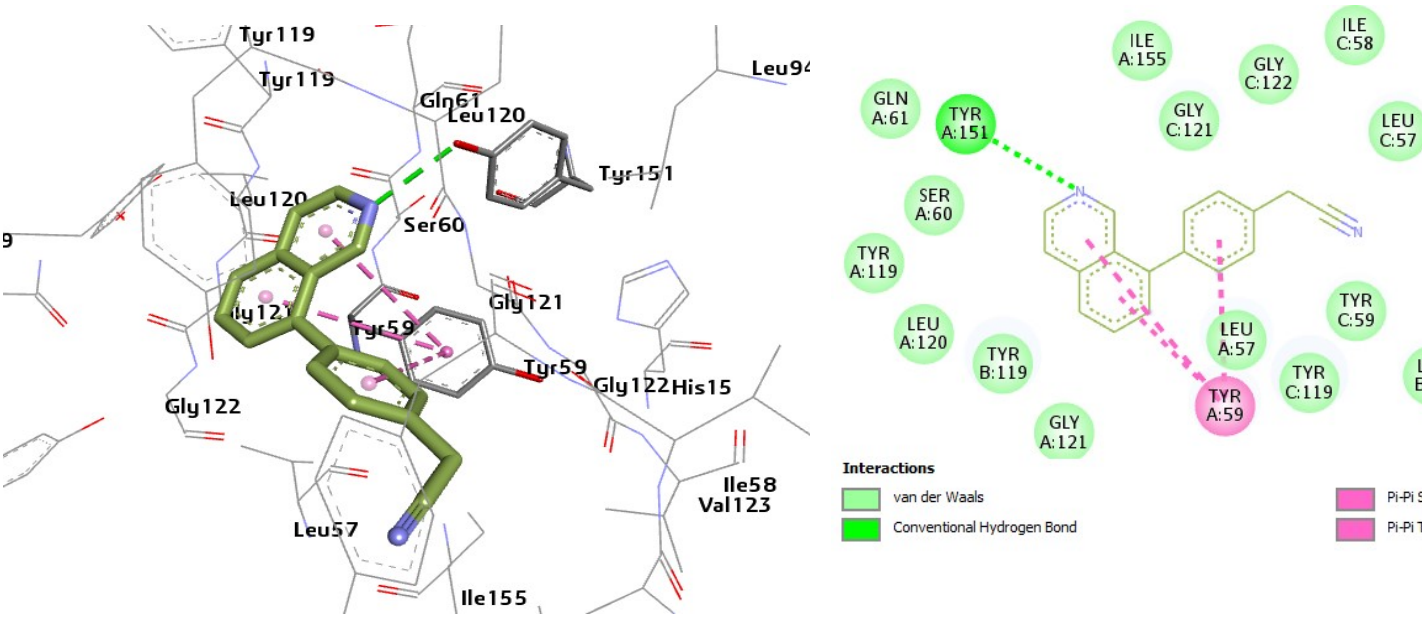
Tyr119
Tyr119
Gln61
Leu120
Tyr151
Leu120
Ser60
Gly121
Tyr59
Tyr59
Gly122
His15
Gly122
Ile58
Val123
Leu57
Ile155
ILE A:155
ILE C:58
GLY C:122
GLN A:61
TYR A:151
GLY C:121
LEU C:57
SER A:60
TYR A:119
TYR C:59
LEU A:120
LEU A:57
TYR B:119
TYR C:119
TYR A:59
GLY A:121
Interactions
van der Waals
Conventional Hydrogen Bond

B

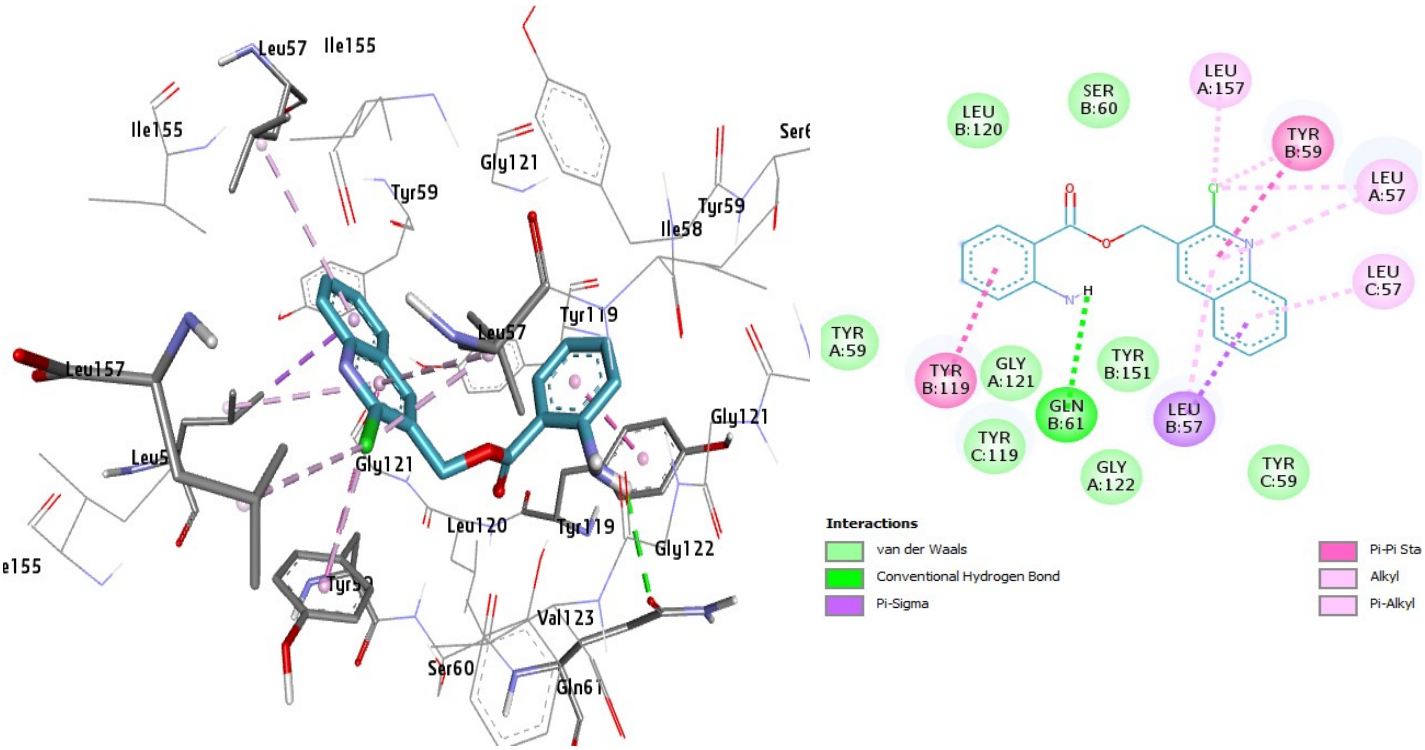
Leu57
Ile155
Ile155
Gly121
Tyr59
Tyr59
Ile58
Tyr119
Leu57
Leu157
Gly121
Gly121
Leu120
Tyr119
Gly122
Ser60
Val123
LEU A:157
SER B:60
LEU B:120
TYR B:59
LEU A:57
LEU C:57
TYR A:59
TYR B:119
GLY A:121
TYR B:151
GLN B:61
LEU B:57
TYR C:119
GLY A:122
TYR C:59
Interactions
van der Waals
Conventional Hydrogen Bond
Pi-Sigma
Alkyl
Pi-Alkyl

C

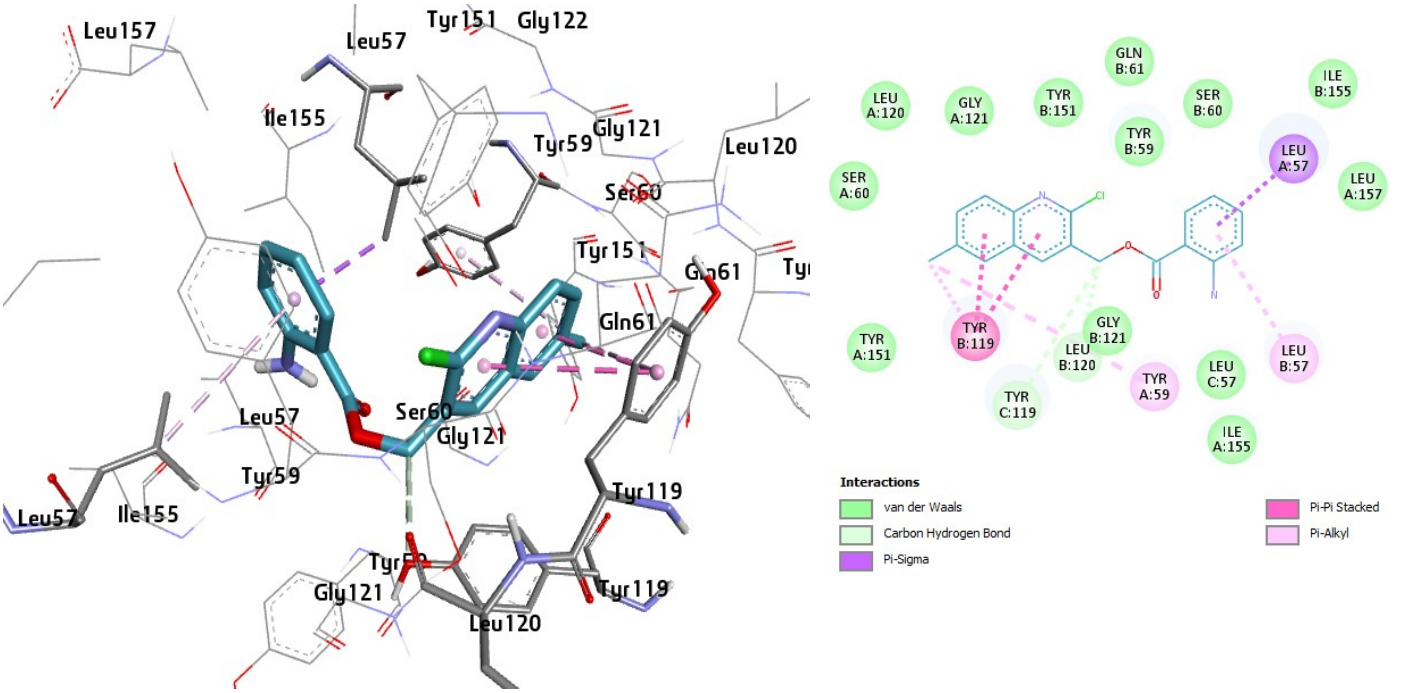

D

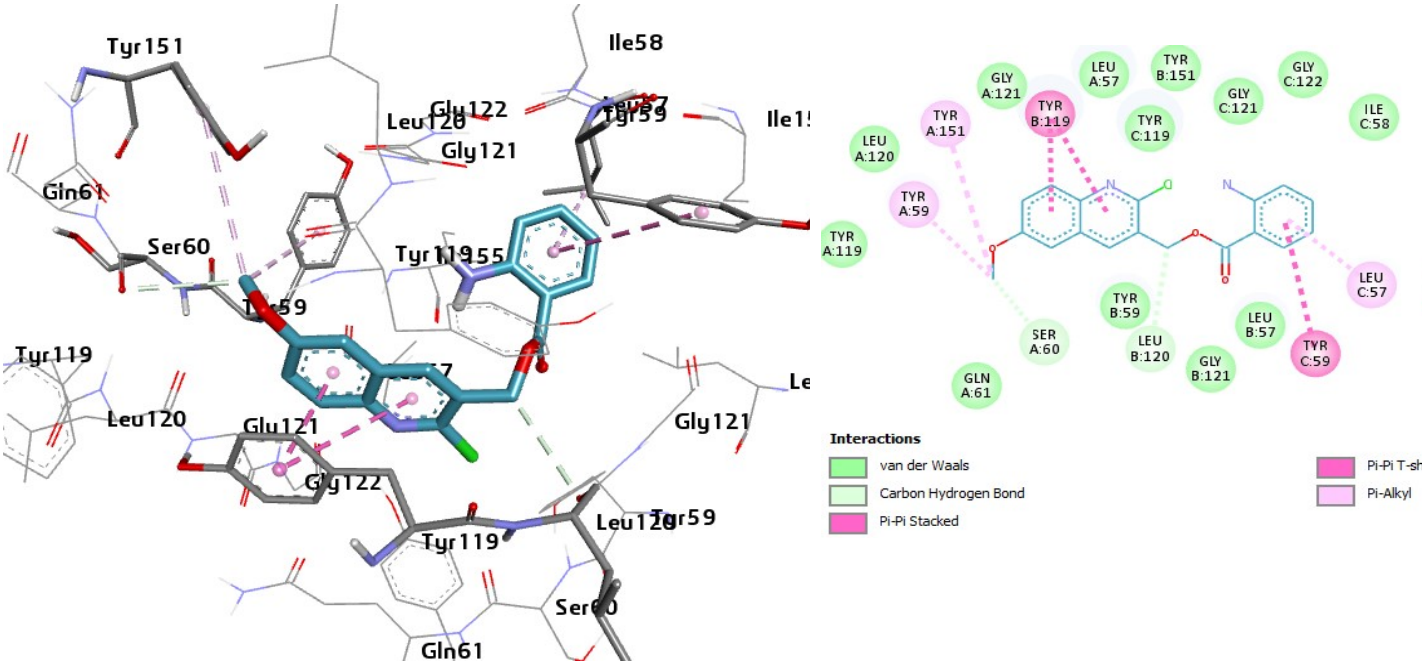

Figure S2. 3D and 2D images of ligand UTJ (A), 5a (B), 5b (C), and 5c (D) docked with Tumor necrosis factor (TNF-α)

A

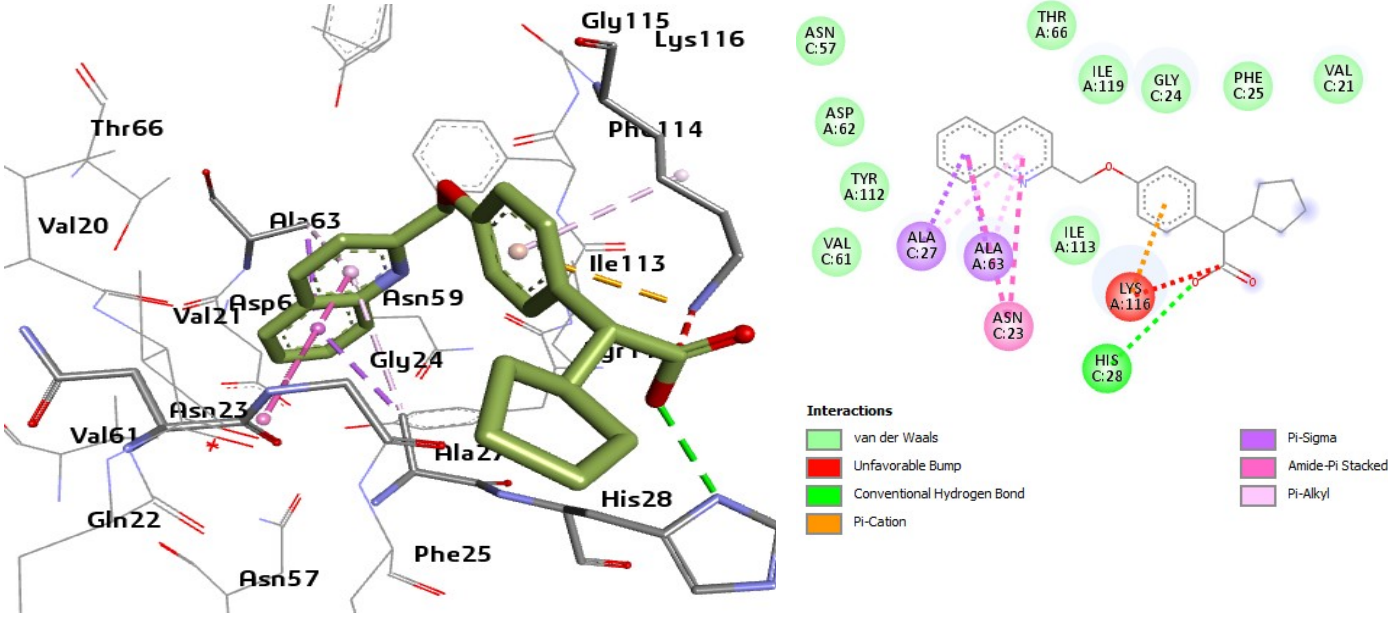
Gly115
Lys116
Thr66
Phe114
Val20
Ala63
Ile113
Val21
Asp62
Asn59
Gly24
Asn23
Val61
Ala27
His28
Gln22
Phe25
Asn57
ASN C:57
THR A:66
ILE A:119
GLY C:24
PHE C:25
VAL C:21
ASP A:62
TYR A:112
VAL C:61
ALA C:27
ALA A:63
ILE A:113
LYS A:116
ASN C:23
HIS C:28
Interactions
van der Waals
Unfavorable Bump
Conventional Hydrogen Bond
Pi-Cation
Pi-Sigma
Amide-Pi Stacked
Pi-Alkyl

B

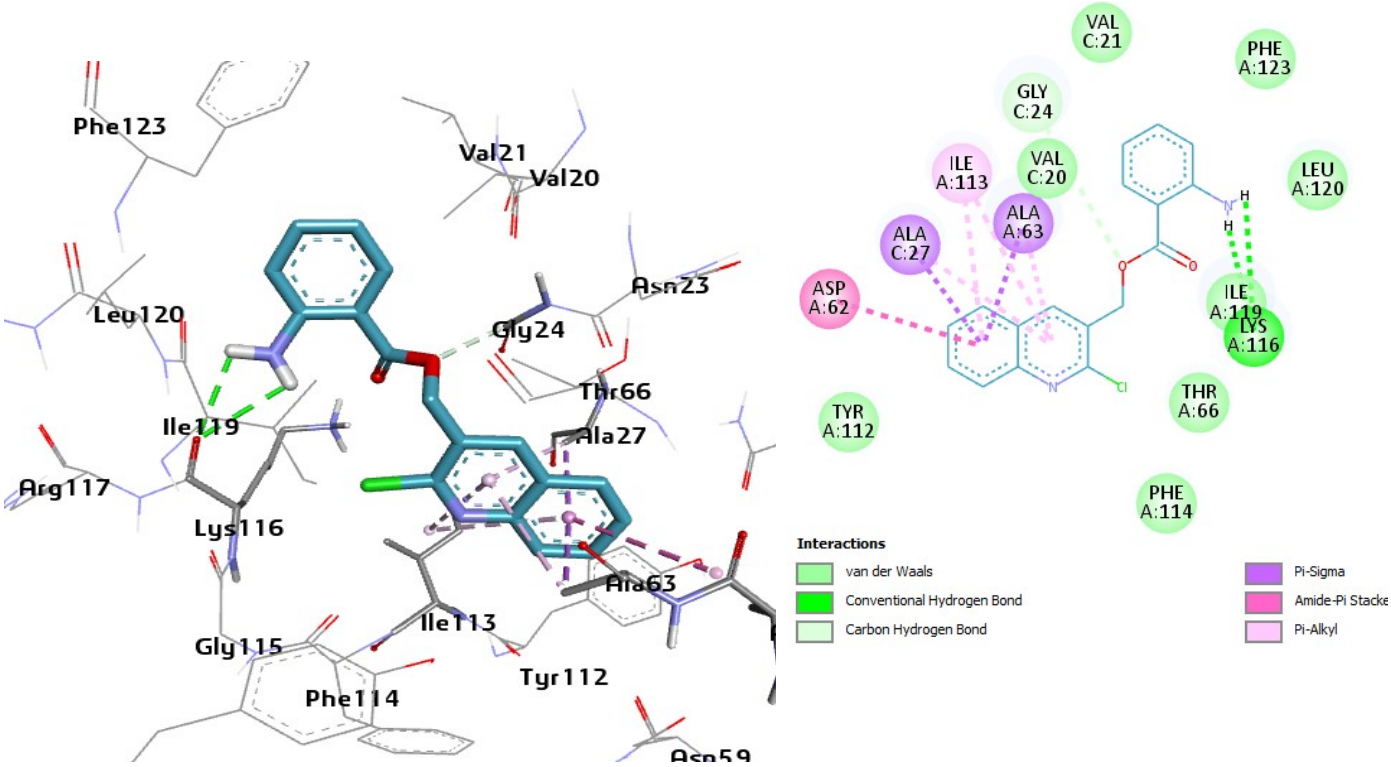
Phe123
Val21
Val20
Asn23
Leu120
Gly24
Thr66
Ile119
Ala27
Arg117
Lys116
Ala63
Ile113
Gly115
Tyr112
Phe114
VAL C:21
PHE A:123
GLY C:24
ILE A:113
VAL C:20
LEU A:120
ALA A:63
ALA C:27
ASP A:62
ILE A:119
LYS A:116
THR A:66
TYR A:112
PHE A:114
Interactions
van der Waals
Conventional Hydrogen Bond
Carbon Hydrogen Bond
Pi-Sigma
Amide-Pi Stacke
Pi-Alkyl

C

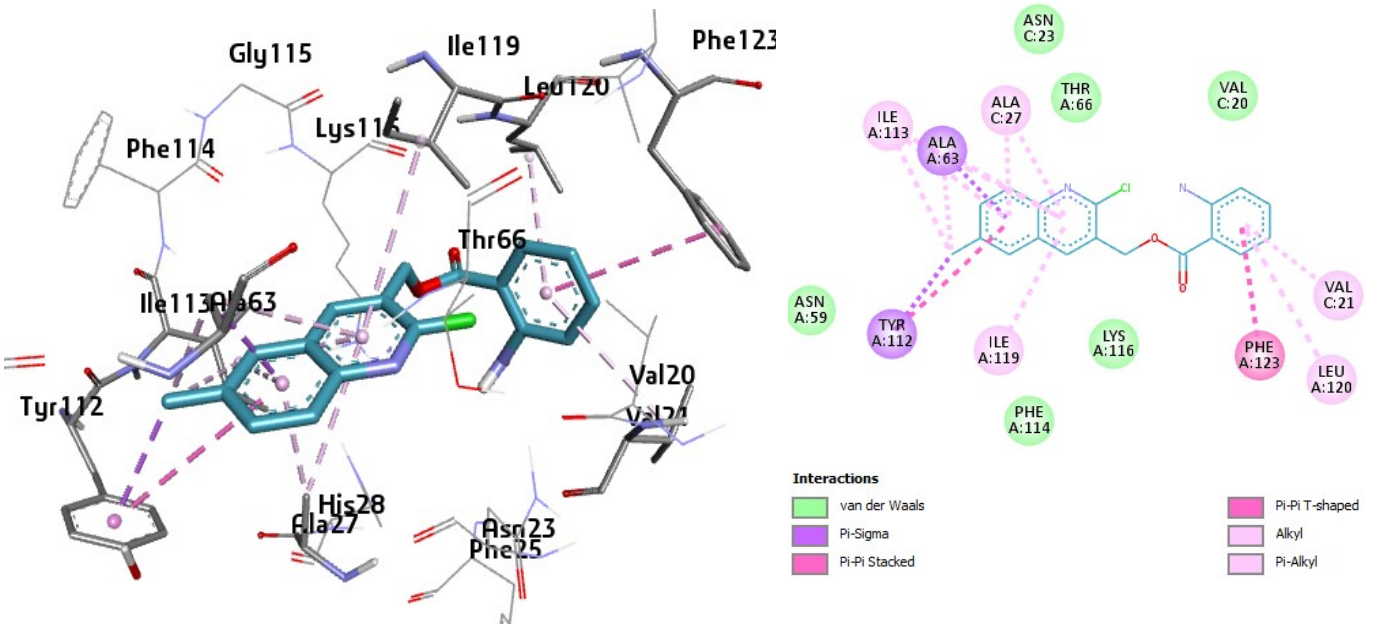

D

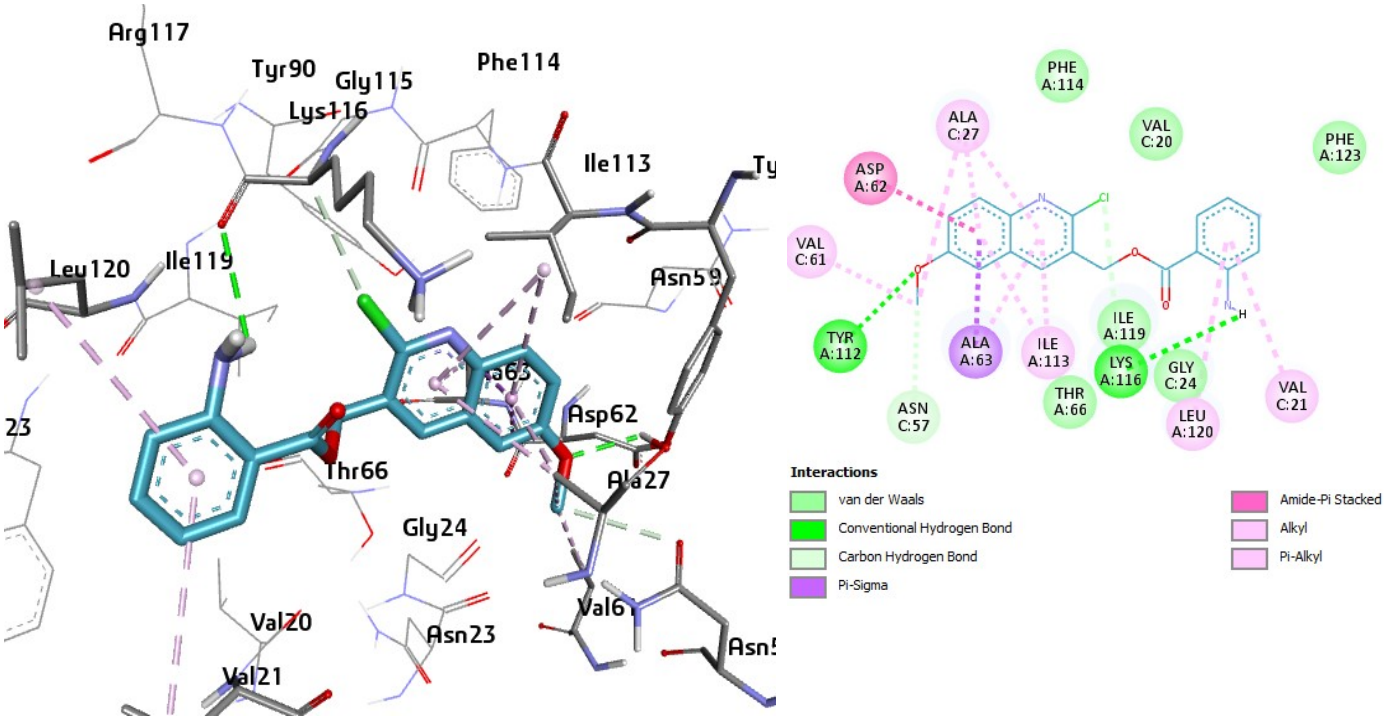

Figure S3. 3D and 2D image of ligand QY1 (A), 5a (B), 5b (C) and 5c (D) docked with 5-Lipoxygenase activating protein (FLAP)

A

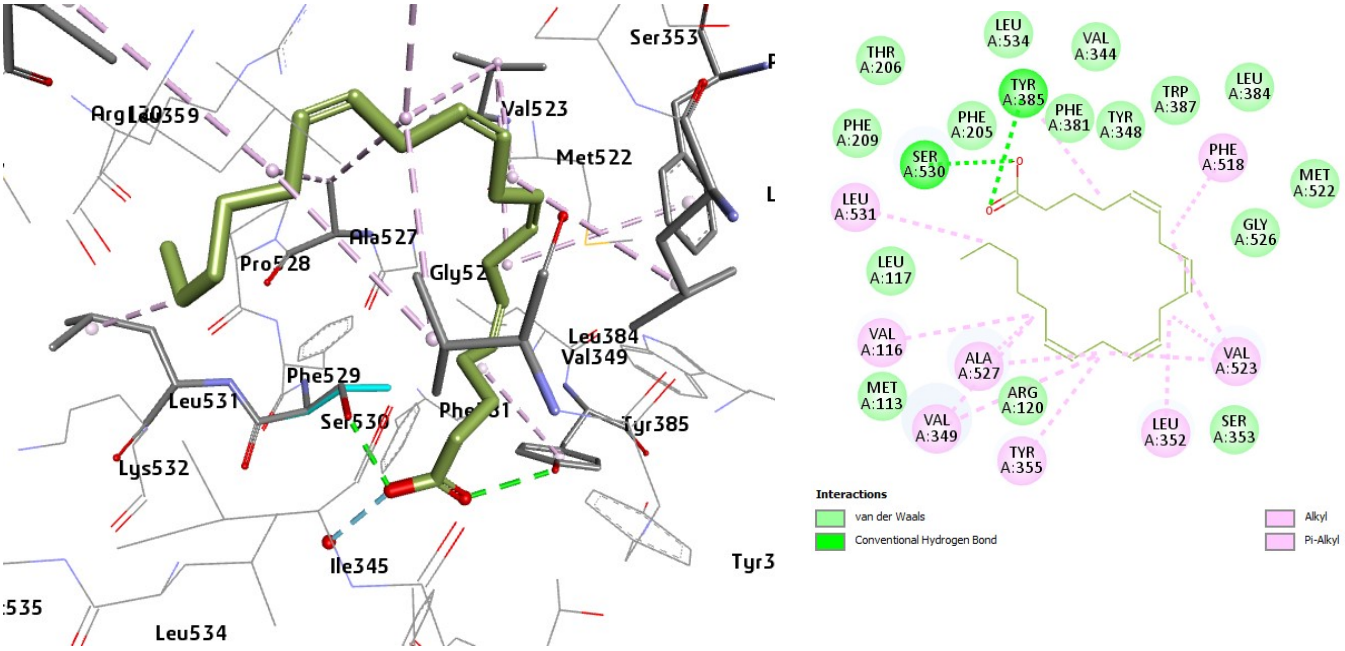
Ser353
Arg120359
Val523
Met522
Ala527
Pro528
Gly52
Leu384
Val349
Phe529
Leu531
Ser530
Phe381
Tyr385
Lys532
Ile345
Tyr3
:535
Leu534
LEU A:534
VAL A:344
THR A:206
TYR A:385
TRP A:387
LEU A:384
PHE A:209
PHE A:205
PHE A:381
TYR A:348
SER A:530
PHE A:518
MET A:522
LEU A:531
GLY A:526
LEU A:117
VAL A:116
ALA A:527
VAL A:523
MET A:113
ARG A:120
VAL A:349
LEU A:352
SER A:353
TYR A:355
Interactions
van der Waals
Conventional Hydrogen Bond
Alkyl
Pi-Alkyl

B

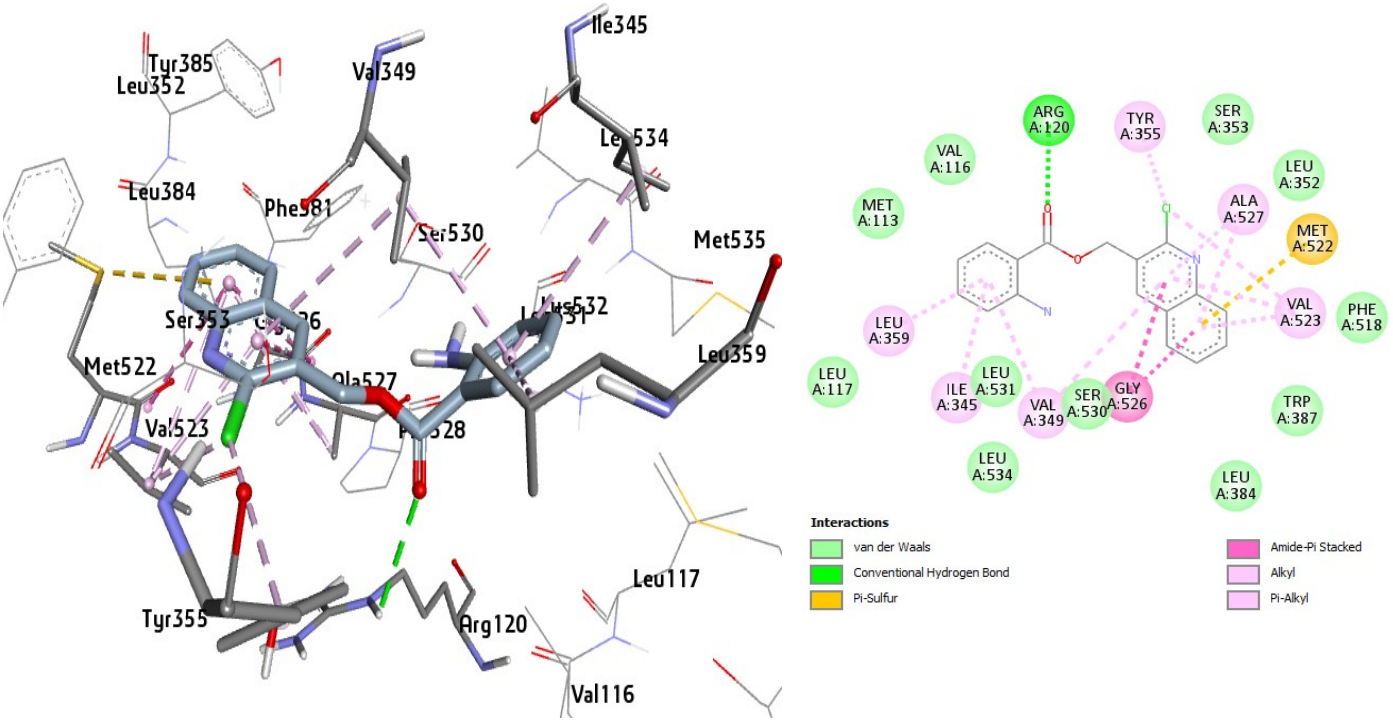
Tyr385
Leu352
Val349
Ile345
Leu534
Leu384
Phe381
Ser530
Met535
Ser353
Lys532
Met522
Leu359
Val523
Tyr355
Arg120
Leu117
Val116
ARG A:120
TYR A:355
SER A:353
VAL A:116
LEU A:352
MET A:113
ALA A:527
MET A:522
LEU A:359
VAL A:523
PHE A:518
LEU A:117
ILE A:345
LEU A:531
VAL A:349
SER A:530
GLY A:526
TRP A:387
LEU A:534
LEU A:384
Interactions
van der Waals
Conventional Hydrogen Bond
Pi-Sulfur
Amide-Pi Stacked
Alkyl
Pi-Alkyl

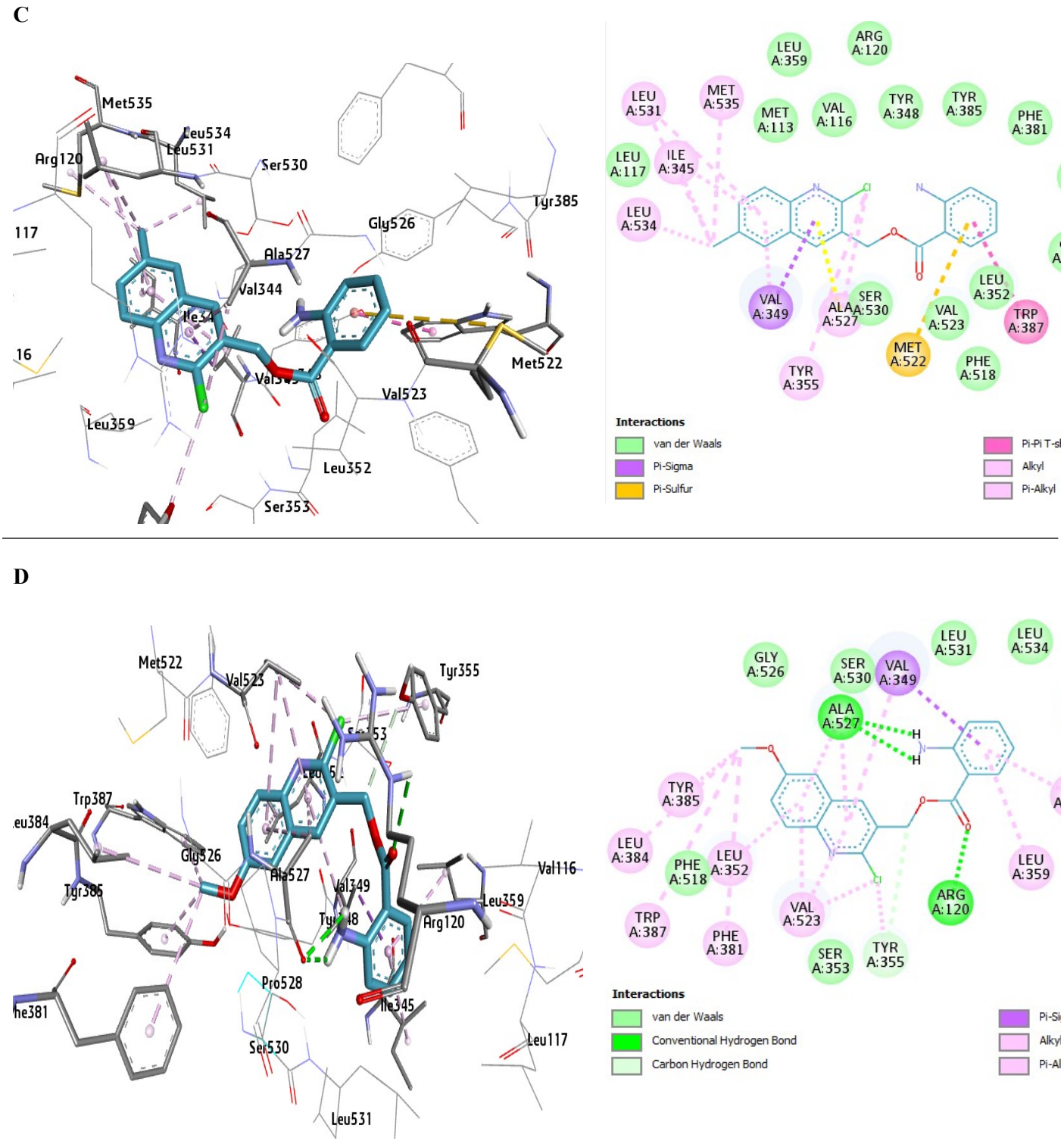

Figure S4. 3D and 2D images of ligands a) ACD (A), 5a (B), 5b (C) and 5c (D) docked with Cyclooxygenase-II (COX-II)

4 Experimental Data

4.1 Synthesis of Compounds

4.1.1 Synthesis of acetamides (L/T/A)[1]

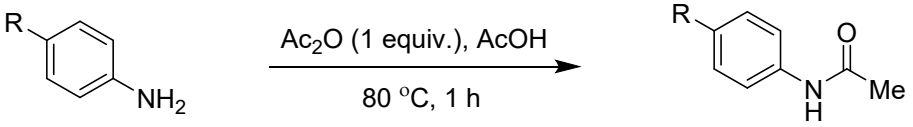

R=H/CH_3/OCH_3

L (R=H)
T (R=CH_3)
A (R=OCH_3)

Substrate (1.0 g *p*-anisidine/*p*-toluidine/aniline) was taken in a round bottom flask, to which 1 equivalent of acetic anhydride and 2 equivalents of glacial acetic acid were added. The reaction mixture was then stirred and heated at 80 °C with constant stirring. Reaction progress was monitored by thin-layer chromatography (TLC). After 1 h, upon completion, the reaction mixture was poured into ice cold water (200ml) and the product (L/T/A), in the form of precipitates, was filtered, washed with water and air-dried.

L: *N*-Phenylacetamide, **yield** (1.26 g, 87%); $\mathbf{R_f}$ (EtOAc:hexane 2:3) 0.39; **m.p.** 113–115°C, Lit.[2] **m.p.** 112–114 °C; IR (neat, cm^{-1}) 3070, 2913, 1663, 1654, 1617, 1591, 1458.

T: *N*-(p-Tolyl)acetamide, **yield** (1.22 g, 88%); $\mathbf{R_f}$ (EtOAc:hexane 2:3) 0.32; **m.p.** 146–148 °C, Lit.[1] **m.p.** 147–148 °C; IR (neat, cm^{-1}) 3123, 3068, 2968, 1661, 1654, 1600, 1456, 1497, 1320.

A: *N*-(4-Methoxyphenyl) acetamide, yield (1.14 g, 85%); $\mathbf{R_f}$ (EtOAc:hexane 2:3) 0.21; **m.p.** 128–130 °C; IR (neat, cm^{-1}) 3064, 2960, 2836,1647, 1600,1464, 1456, 1367, 1242, 1028.

4.1.2 Synthesis of 1(a-c)[3]

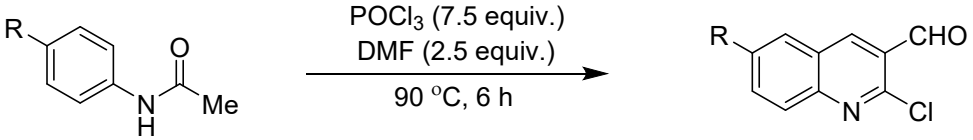

L (R=H)
T (R=CH_3)
A (R=OCH_3)

1a (R=H)
1b (R=CH_3)
1c (R=OCH_3)

To the round bottom flask, *N*-*N*-dimethylformamide (2.5 equiv.) was added and stirred over an ice bath. Keeping the temperature at 0 °C, $POCl_3$ (7.5 equiv.) was added dropwise in 0.5 h, and after complete addition the *N*-acetamide (A/T/L) was added and the reaction mixture was transferred to

the hotplate and refluxed at 90 °C for 6 h over oil bath. Continuous monitoring was done using TLC and after consumption of substrate reaction mixture was allowed to cool a room temperature and then added to crushed ice and stirred again for 30 min. The resulting yellow precipitates were filtered, washed with cold water and air-dried. The crude product was purified by silica gel column chromatography using ethyl acetate and *n*-hexane (1:9) to afford the aldehyde 1(a-c).

2-Chloroquinoline-3-carbaldehyde (1a)

Yield (0.94 g, 66%); $\mathbf{R_f}$ (EtOAc:hexane, 1:4) 0.50; **m.p.** 148–150 °C, Lit.[3] **m.p.** 148–149 °C; **IR** (neat, cm^{-1}) 3060, 1682, 1613, 1576, 1489, 1454, 1390, 748; **^{1}H NMR** (600 MHz, $CDCl_3$) δ 10.56 (s, 1H), 8.76 (s, 1H), 8.07 (d, J = 8.4 Hz, 1H), 7.98 (ddd, J = 8.2, 1.5, 0.5 Hz, 1H), 7.89 (ddd, J = 8.5, 6.8, 1.5 Hz, 1H), 7.65 (ddd, J = 8.2, 6.8, 1.2 Hz, 1H); **^{13}C NMR** (150 MHz, $CDCl_3$) δ 189.3, 150.2, 149.7, 140.4, 133.7, 129.8, 128.7, 128.2, 126.6, 126.5.

2-Chloro-6-methylquinoline-3-carbaldehyde (1b)

Yield (0.90 g, 65%); $\mathbf{R_f}$ (EtOAc:hexane, 1:4) 0.64; **m.p.** 123–125 °C, Lit.[3] **m.p.** 124–125 °C; **IR** (neat, cm^{-1}) 3072, 2952, 2923, 2875, 1686, 1584, 1490, 1457, 735; **^{1}H NMR** (600 MHz, $CDCl_3$) δ 10.54 (s, 1H), 8.66 (s, 1H), 7.96 (d, J = 8.6 Hz, 1H), 7.72 (d, J = 2.0 Hz, 1H), 7.70 (dd, J = 8.6, 2.0 Hz, 1H), 2.56 (s, 3H); **^{13}C NMR** (150 MHz, $CDCl_3$) δ 189.4, 149.4, 148.3, 139.7, 138.5, 136.1, 128.5, 128.3, 126.7, 126.4, 21.6.

2-Chloro-6-methoxyquinoline-3-carbaldehyde (1c)

Yield (0.86 g, 64%); $\mathbf{R_f}$ (EtOAc:hexane, 1:4) 0.52; **m.p.** 144–146 °C, Lit.[3] **m.p.** 145–147 °C; **IR** (neat, cm^{-1}) 3053, 2956, 2870, 1616, 1680, 1571, 1492, 1465, 1395, 1227, 1050, 730.

5 Spectroscopic Data

5.1 ^{1}H NMR ($CDCl_3$, 600 MHz) of 2-Chloroquinoline-3-carbaldehyde (1a)

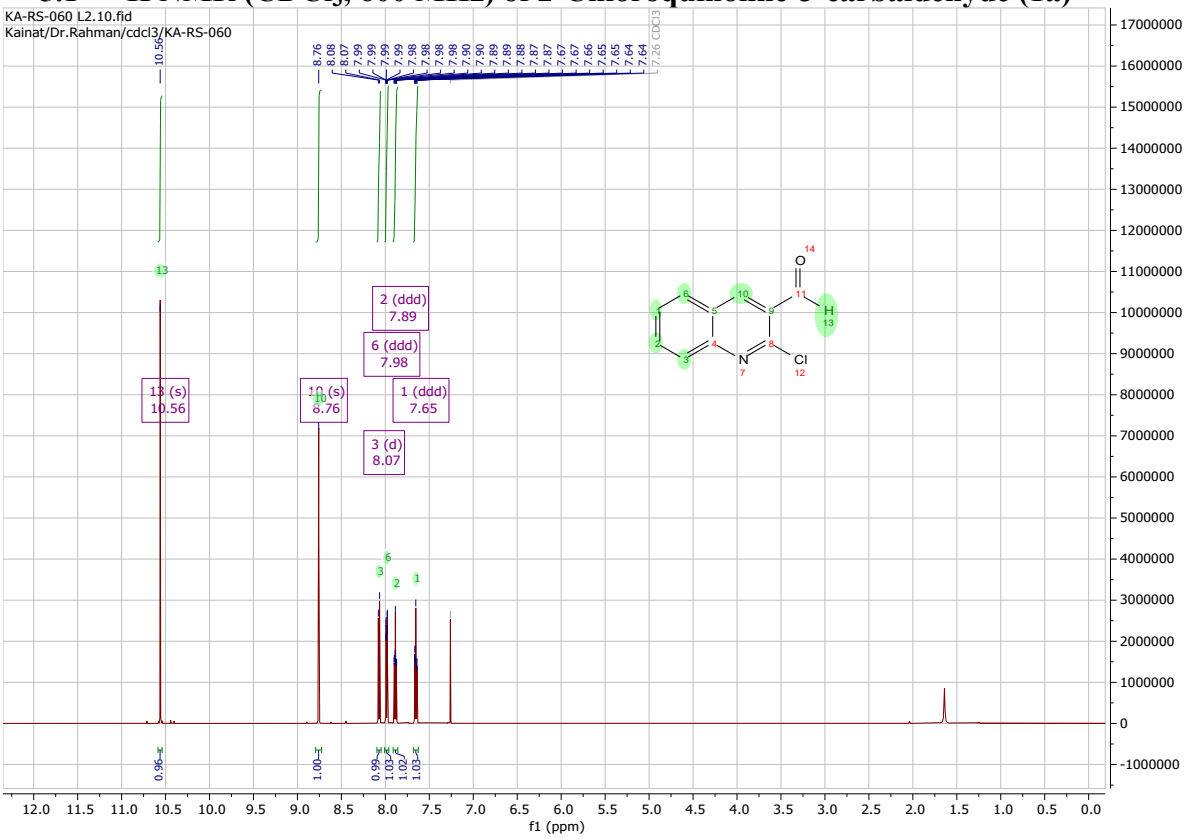

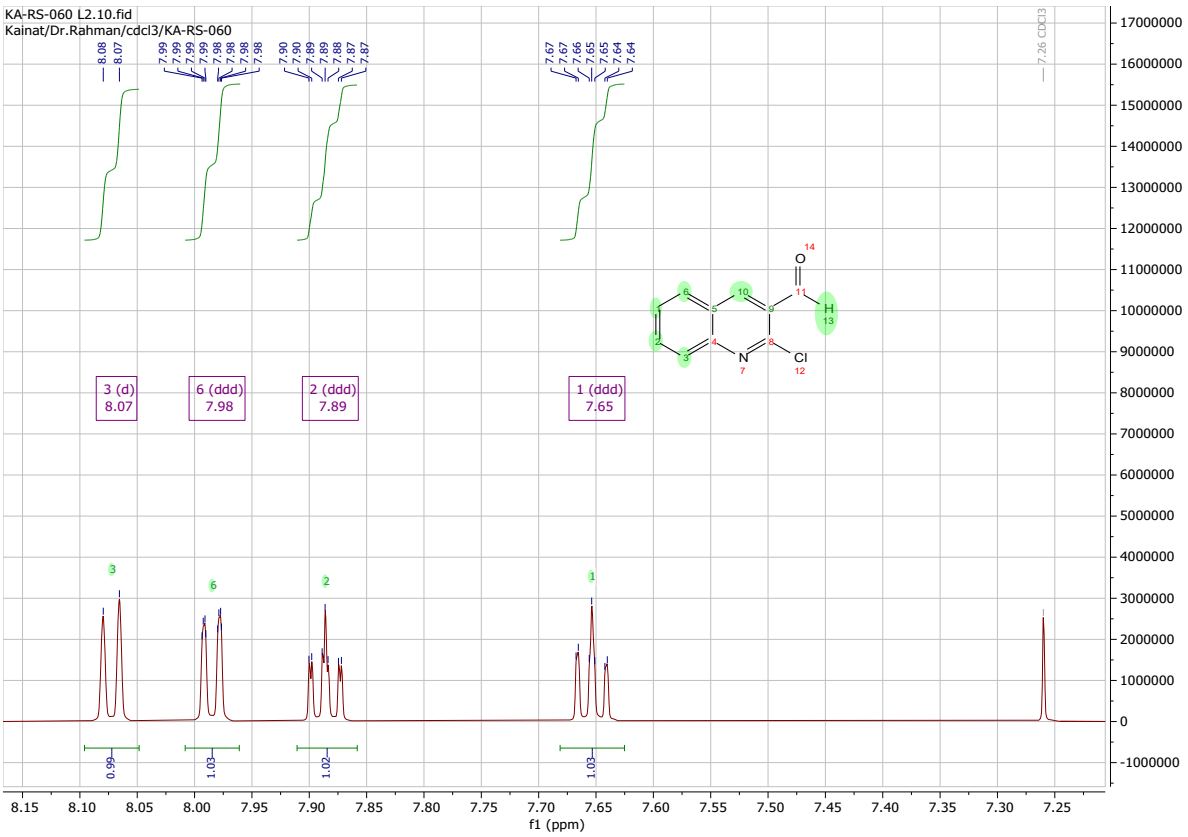

5.2 ^{13}C NMR ($CDCl_3$, 150 MHz) of 2-Chloroquinoline-3-carbaldehyde (1a)

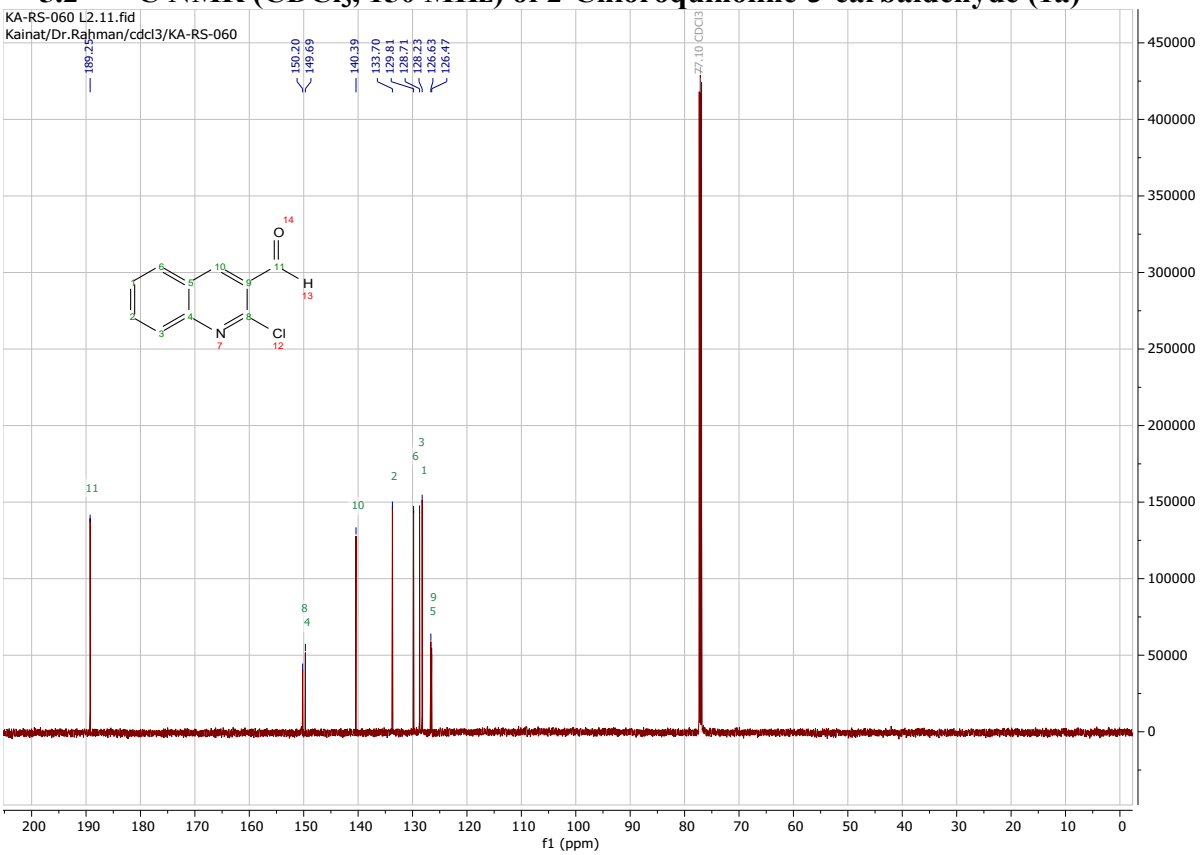

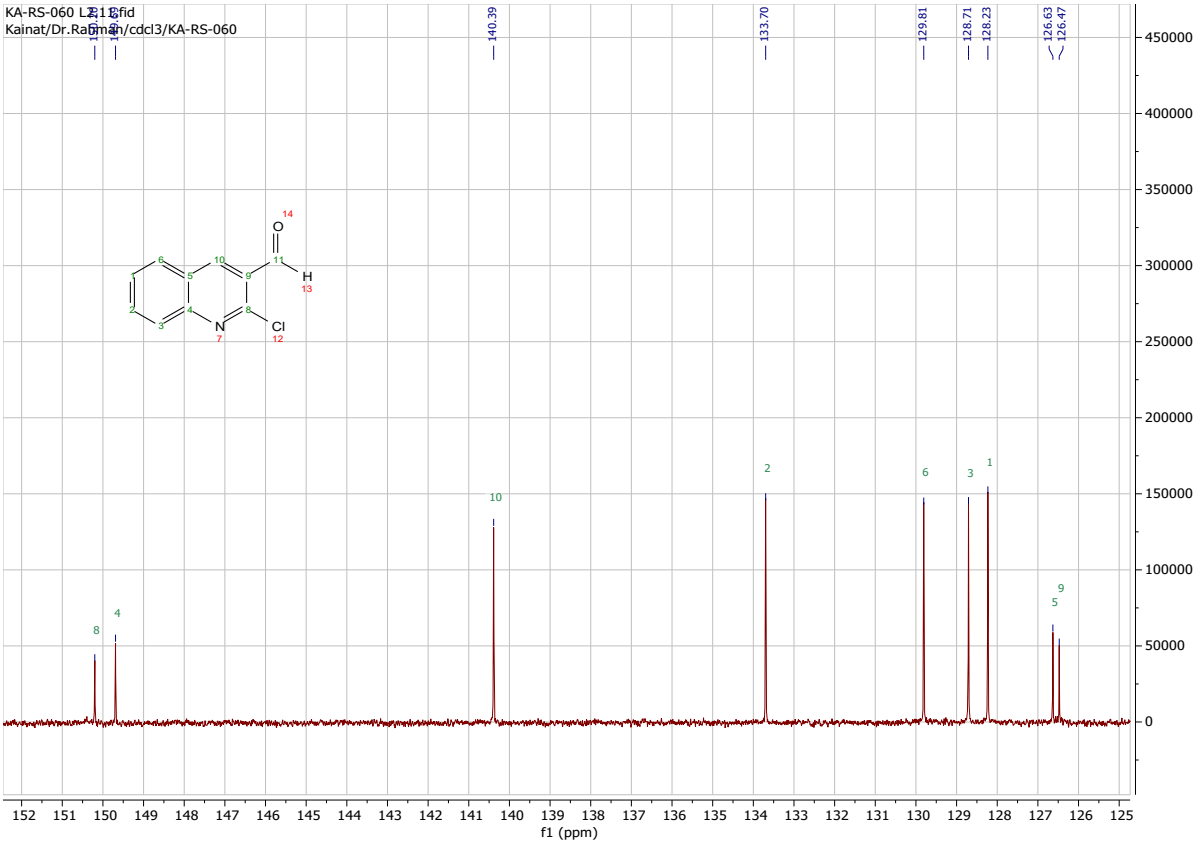

5.3 DEPT-135 NMR ($CDCl_3$, 150 MHz) of 2-Chloroquinoline-3-carbaldehyde (1a)

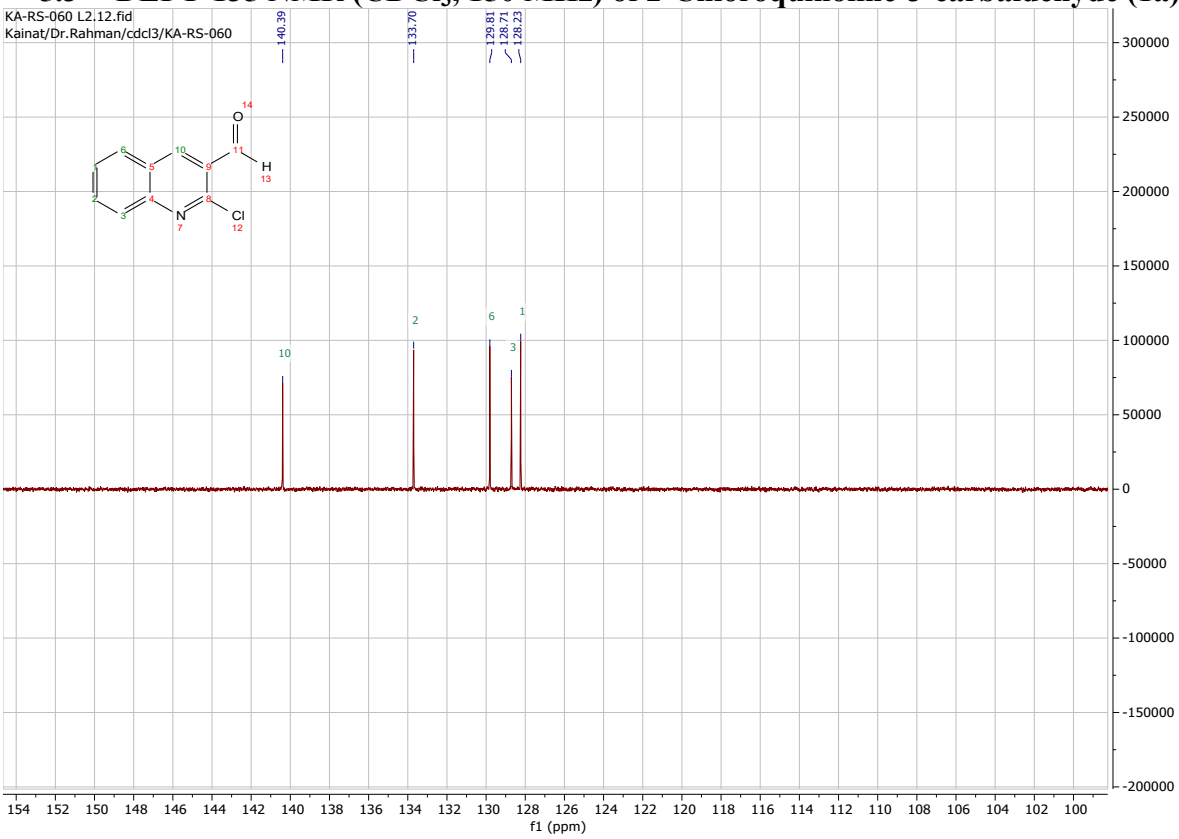

5.4 ^{1}H NMR ($CDCl_3$, 600 MHz) of 2-Chloro-6-methylquinoline-3-carbaldehyde 1b

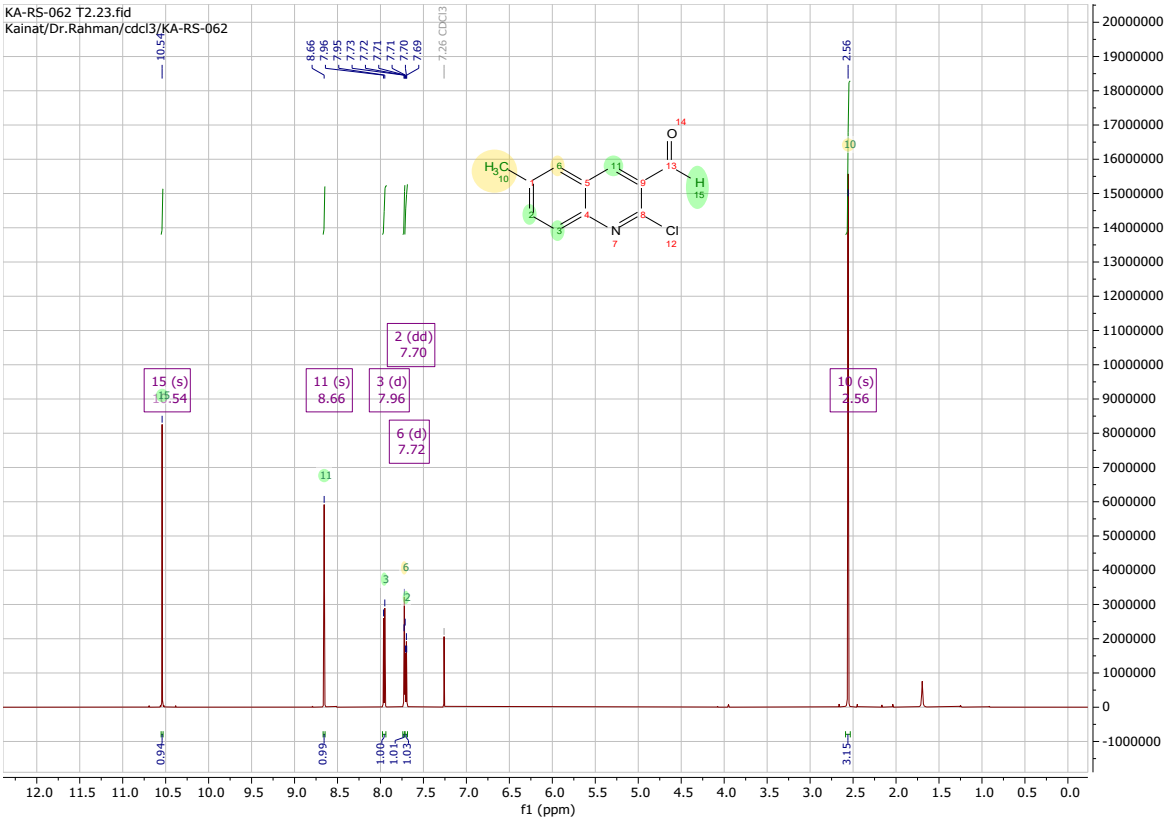

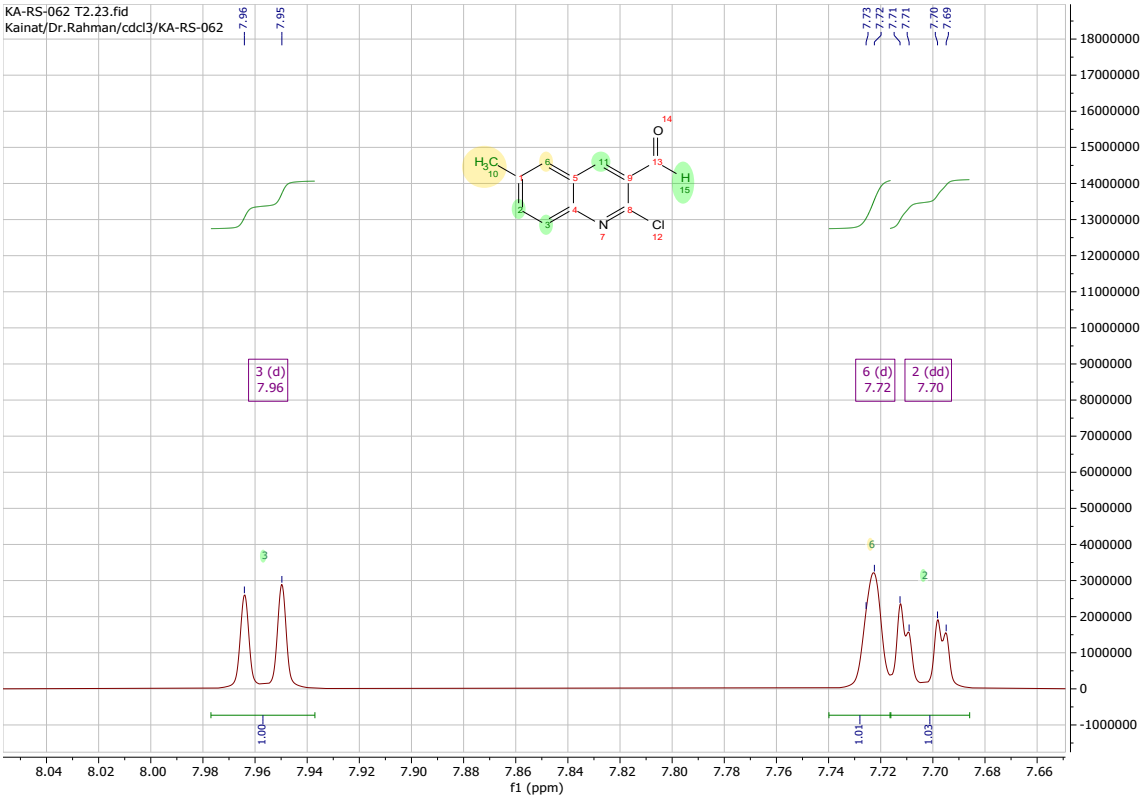

5.5 ^{13}C NMR ($CDCl_3$, 150 MHz) of 2-Chloro-6-methylquinoline-3-carbaldehyde 1b

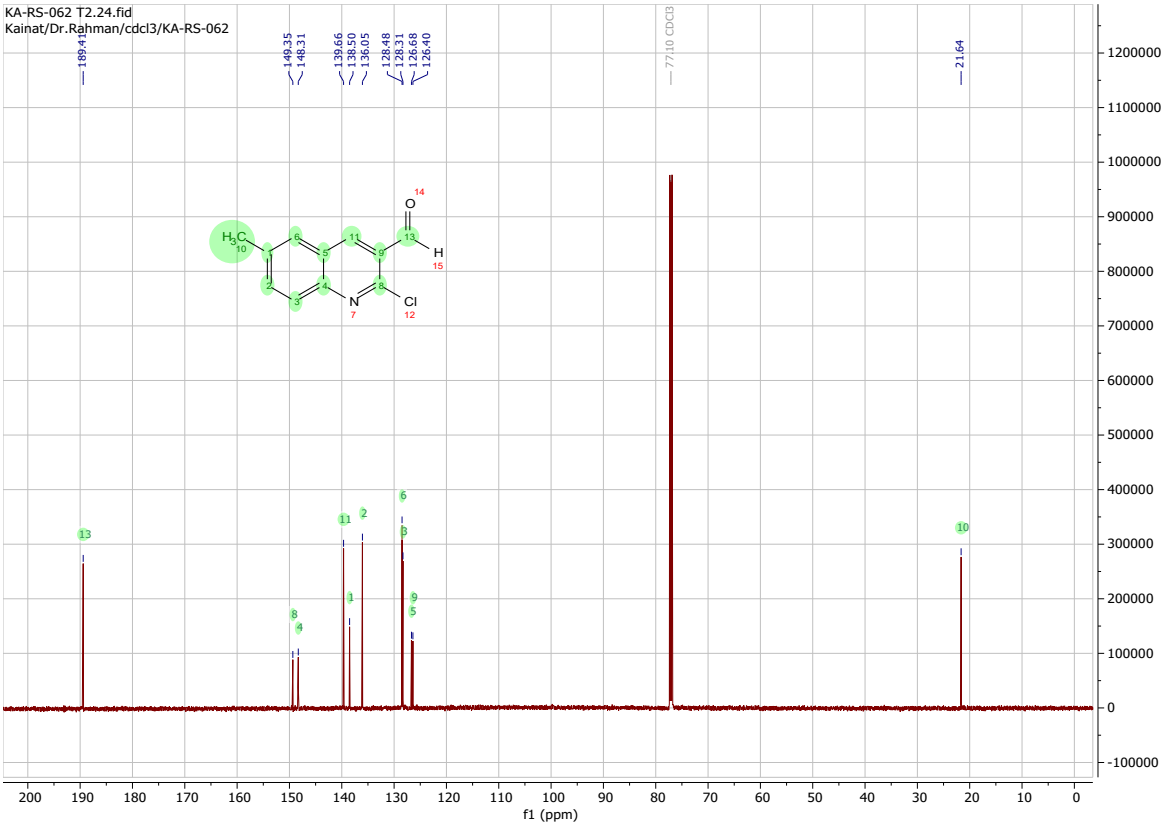

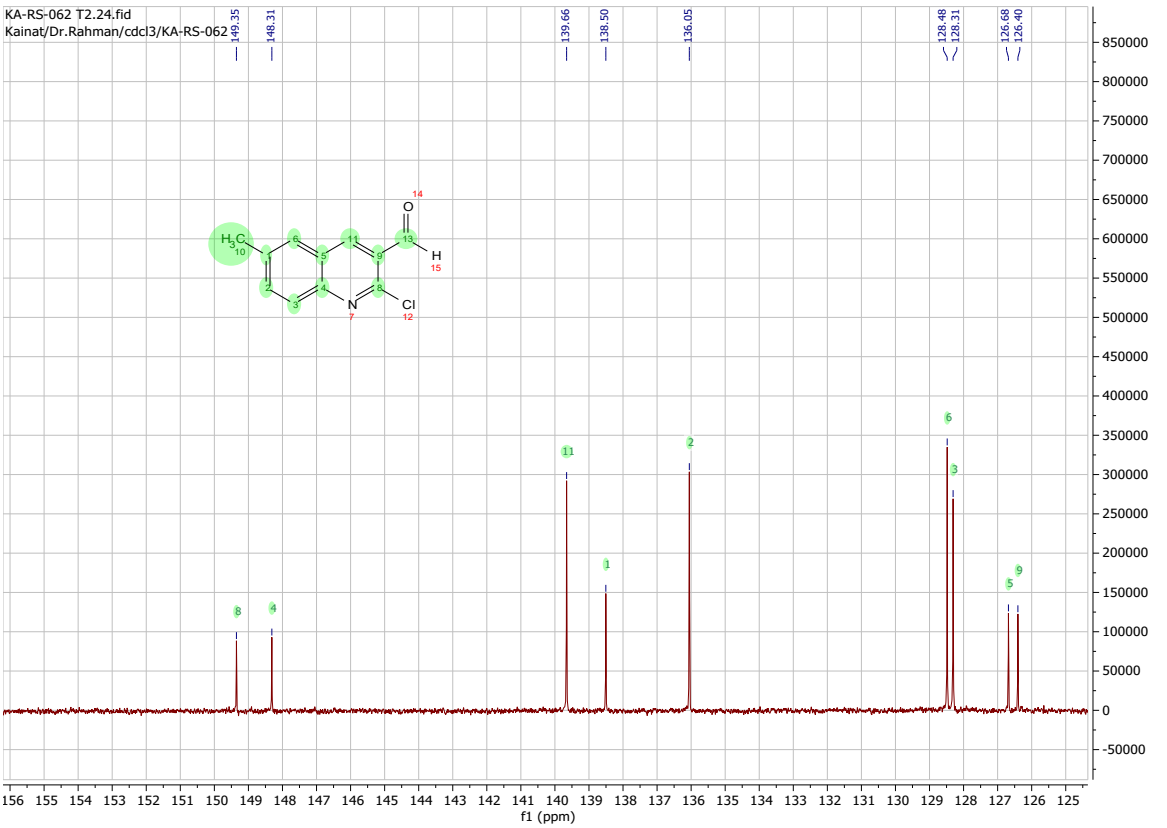

5.6 DEPT-135 NMR ($CDCl_3$, 150 MHz) of 2-Chloro-6-methylquinoline-3-carbaldehyde 1b

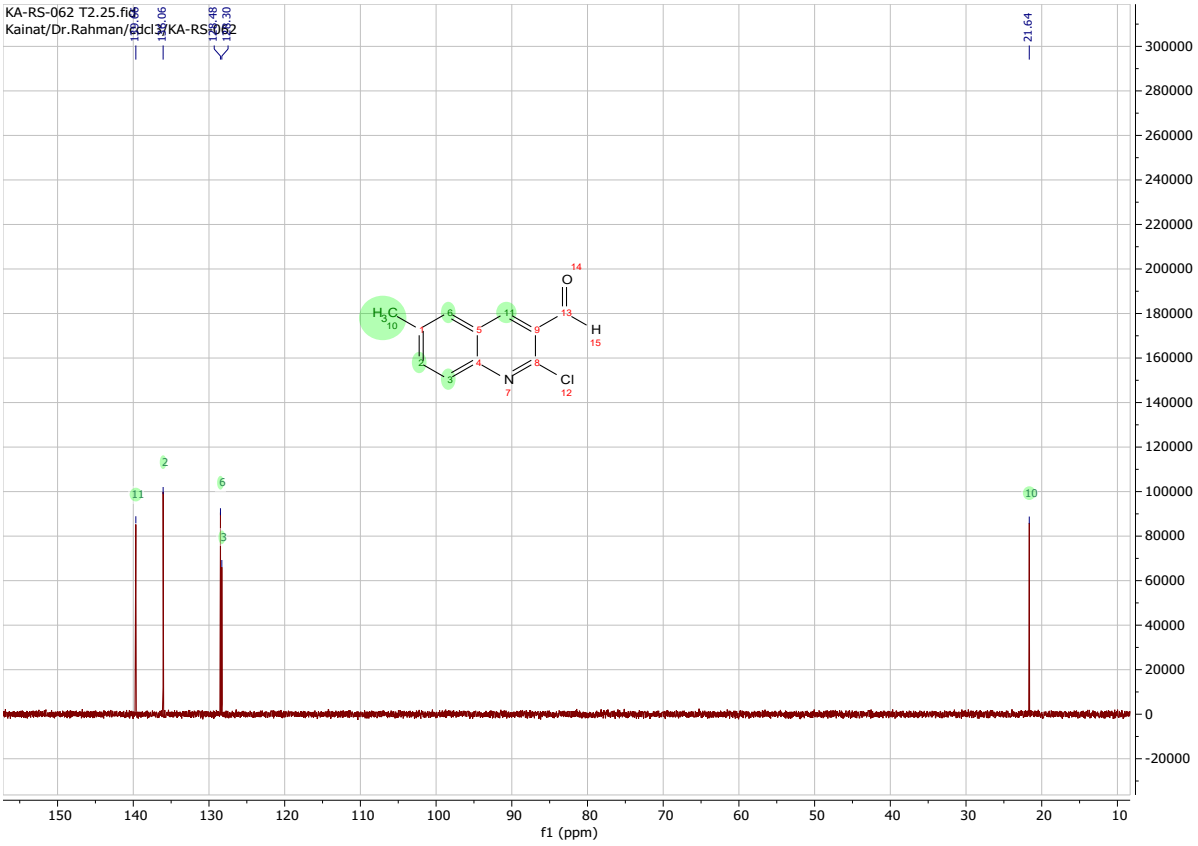

5.7 ^1H NMR ($CDCl_3$, 600 MHz) of (2-Chloroquinolin-3-yl)methanol (2a)

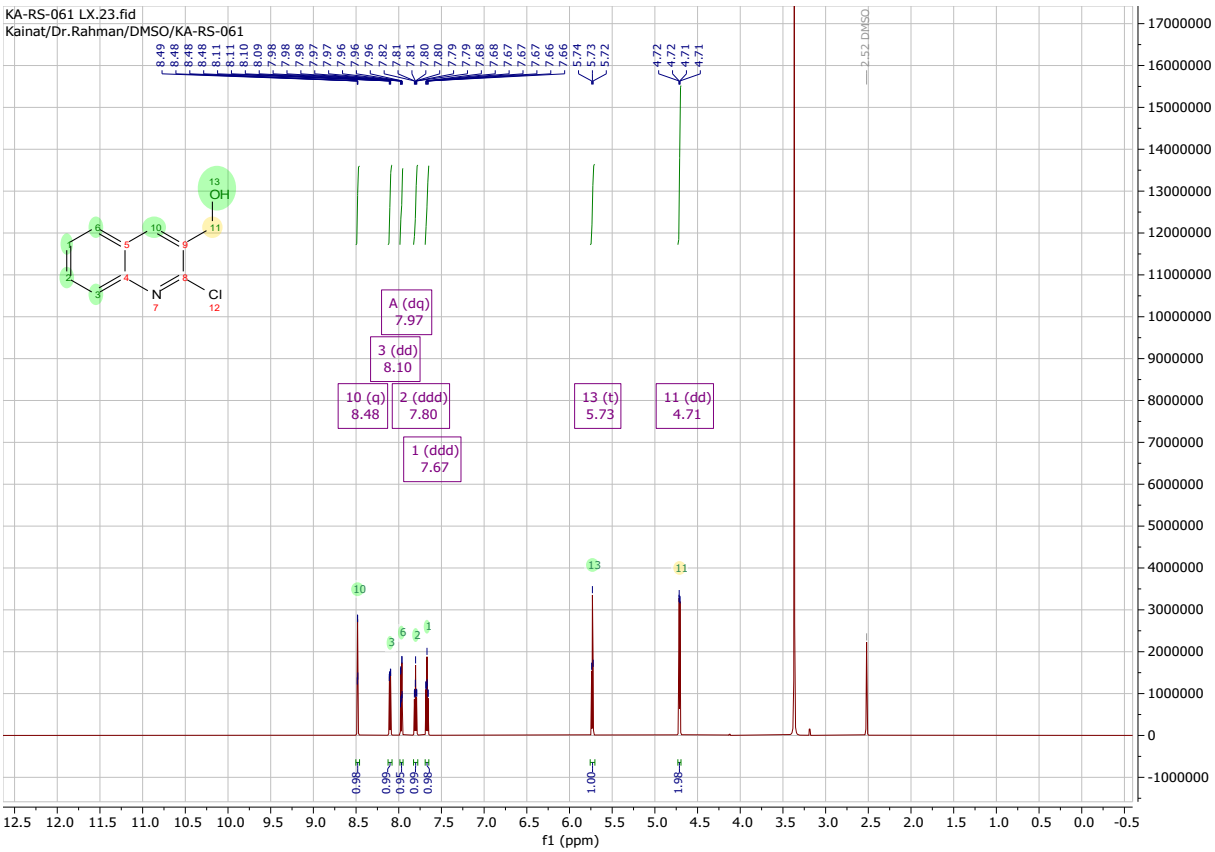
KA-RS-061 LX.23.fid
Kainat/Dr.Rahman/DMSO/KA-RS-061
A (dq)
7.97
3 (dd)
8.10
10 (q)
8.48
2 (ddd)
7.80
1 (ddd)
7.67
13 (t)
5.73
11 (dd)
4.71
2.52 DMSO
f1 (ppm)

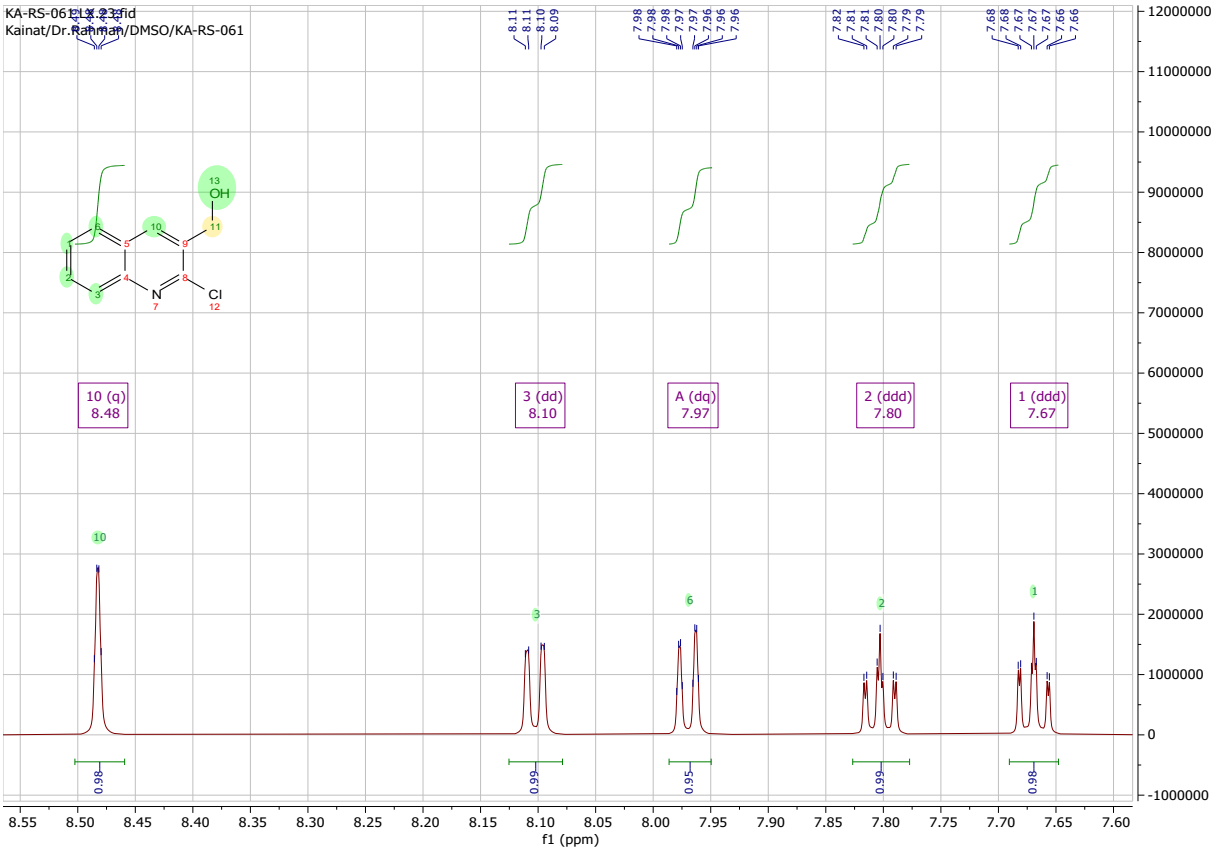
KA-RS-061 LX.23.fid
Kainat/Dr.Rahman/DMSO/KA-RS-061
10 (q)
8.48
3 (dd)
8.10
A (dq)
7.97
2 (ddd)
7.80
1 (ddd)
7.67
f1 (ppm)

5.8 ^{13}C NMR ($CDCl_3$, 150 MHz) of (2-Chloroquinolin-3-yl)methanol (2a)

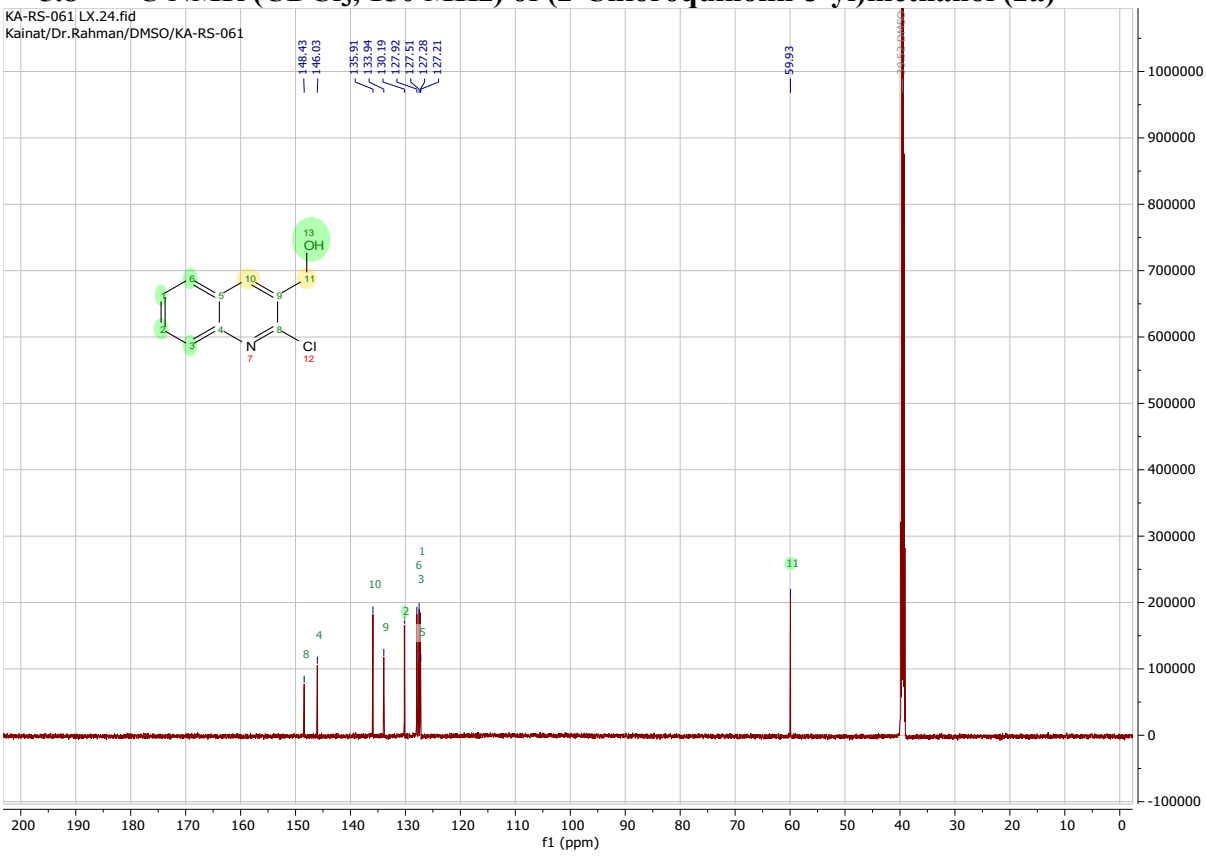

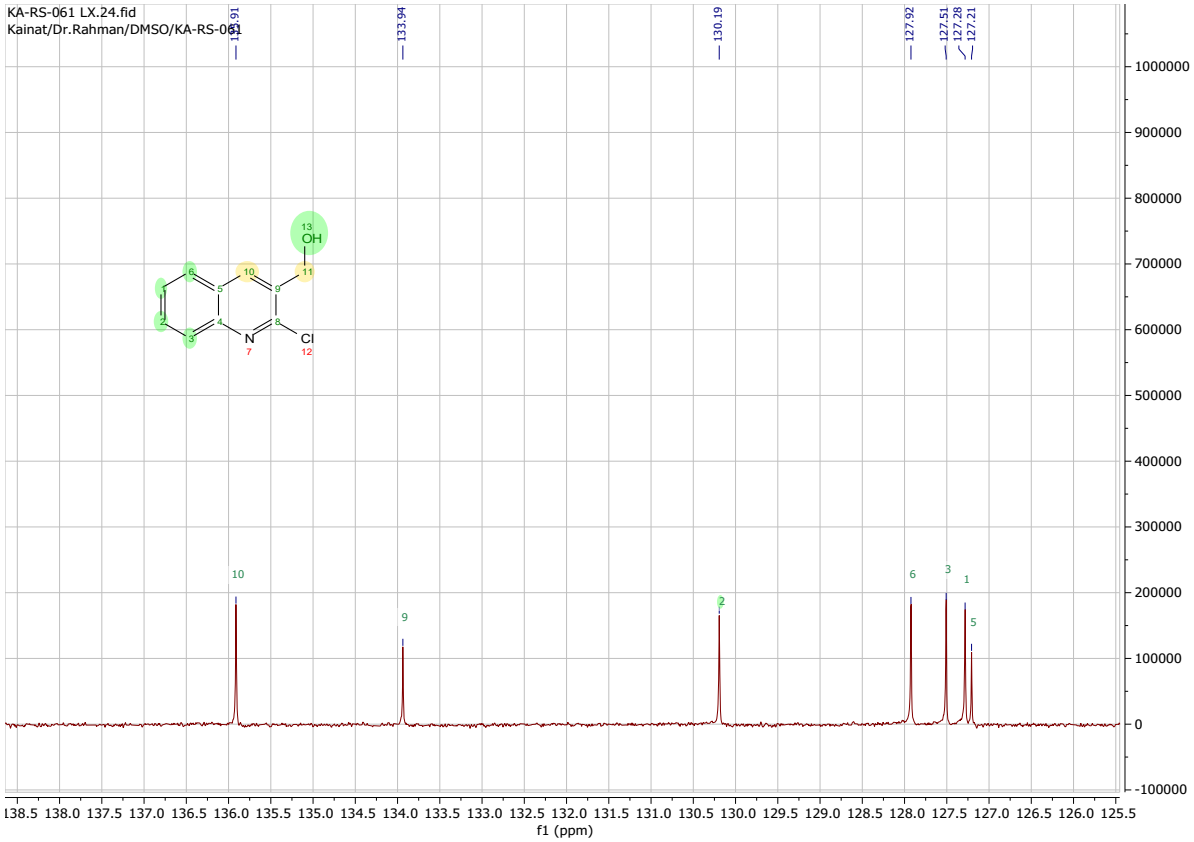

5.9 DEPT-135 NMR ($CDCl_3$, 150 MHz) of (2-Chloroquinolin-3-yl)methanol (2a)

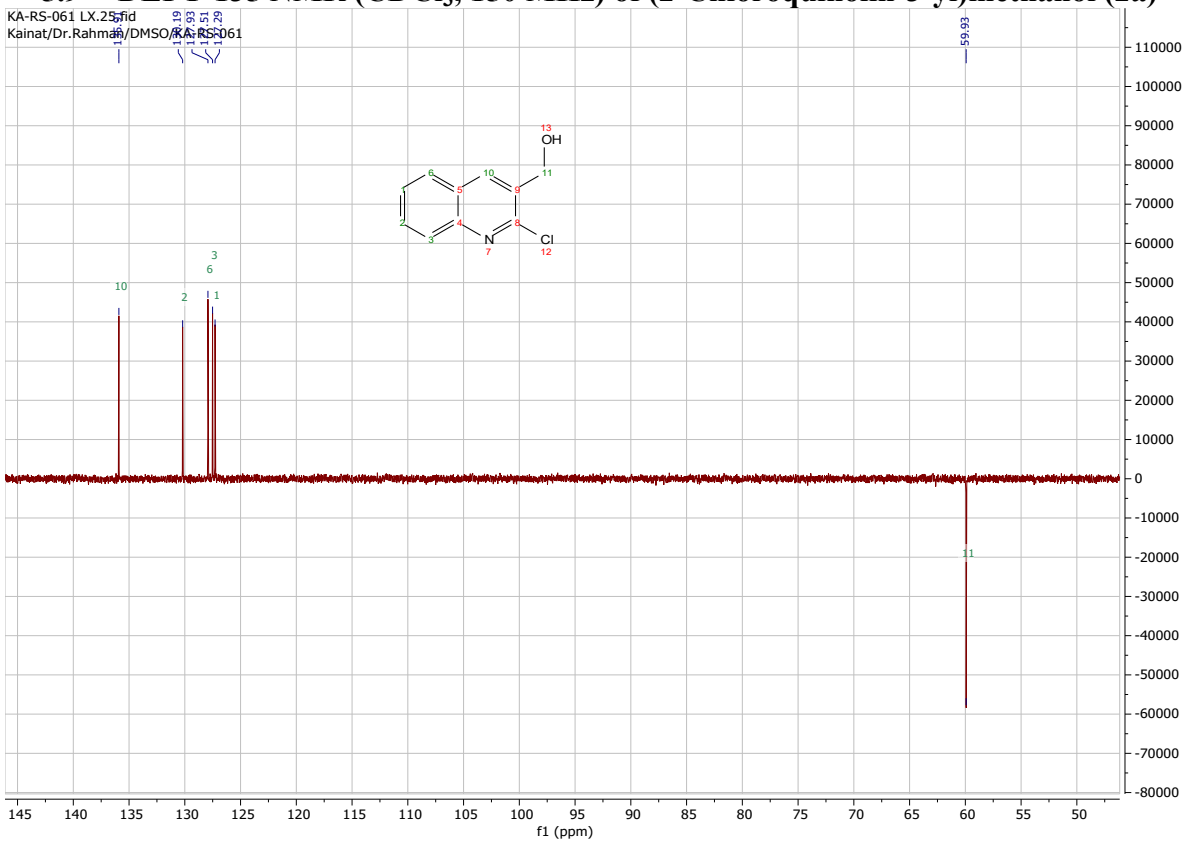

5.10 ^{1}H NMR (DMSO, 600 MHz) of (2-Chloro-6-methylquinolin-3-yl)methanol) (2b)

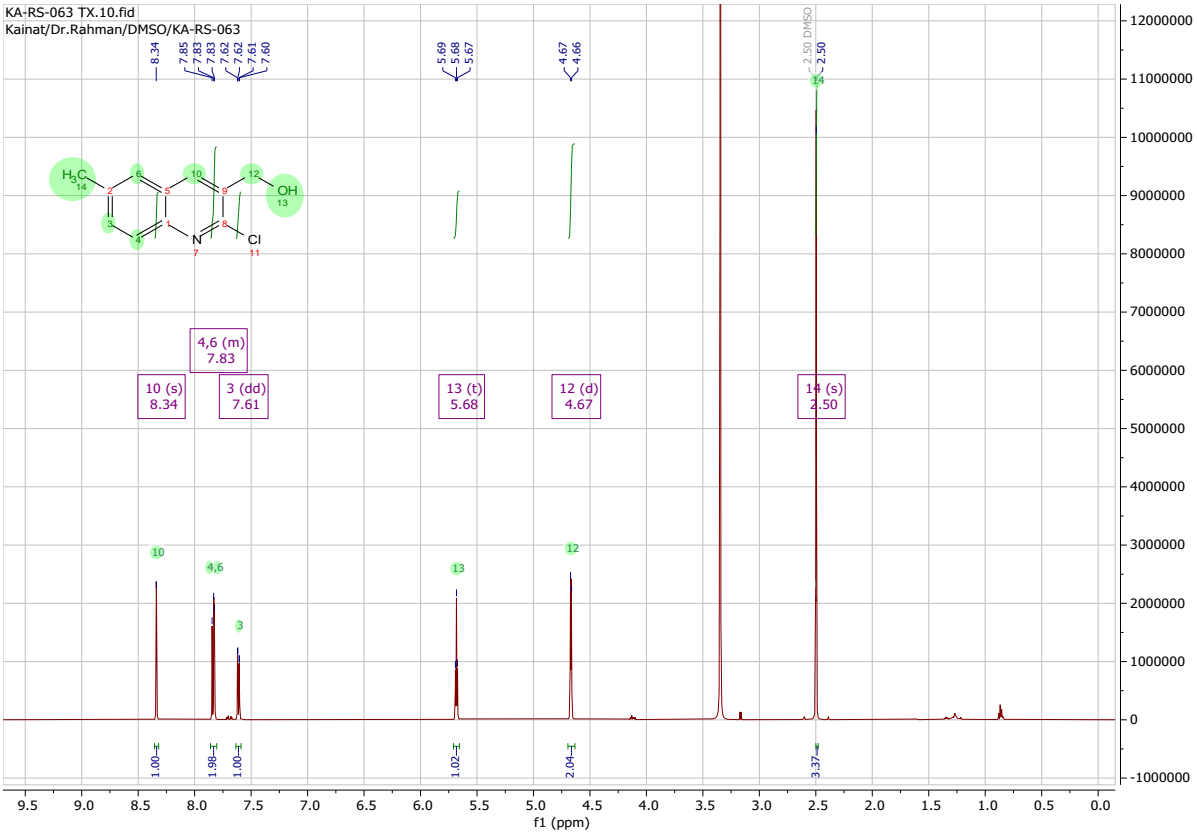

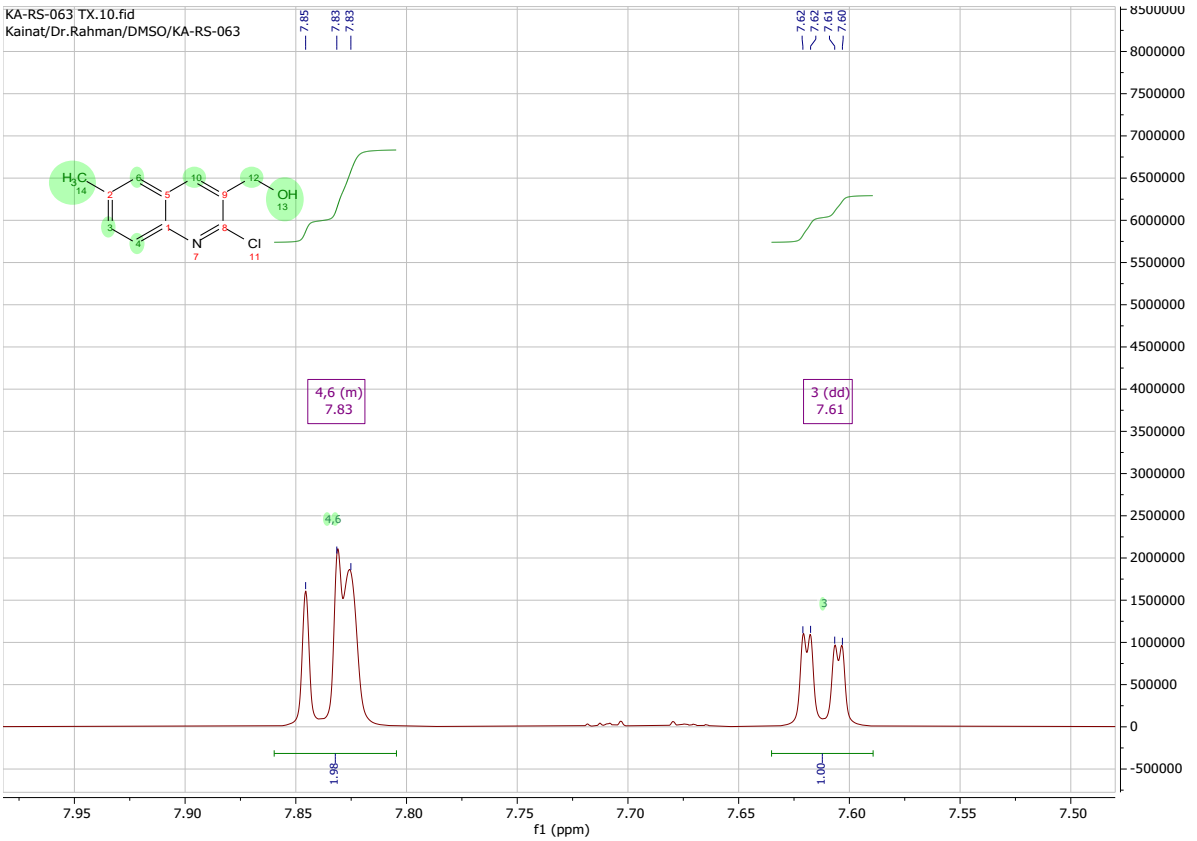

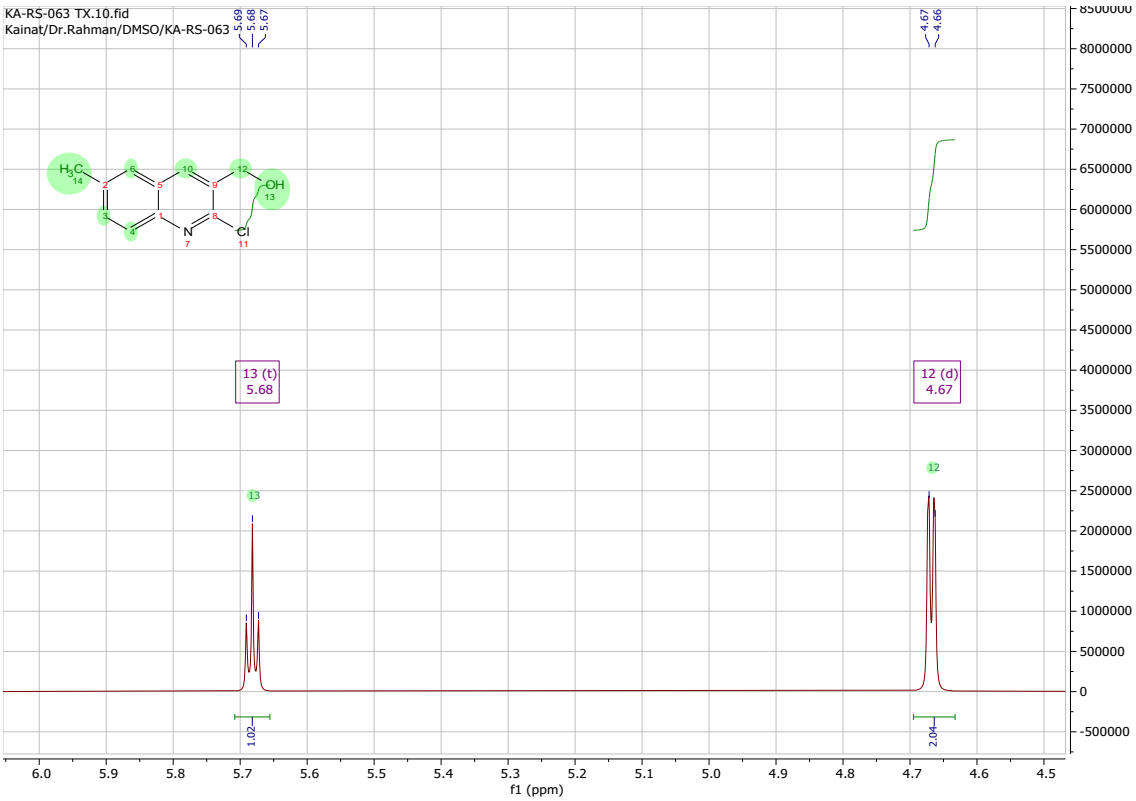

5.11 ^{13}C NMR (DMSO, 150 MHz) of (2-Chloro-6-methylquinolin-3-yl)methanol) (2b)

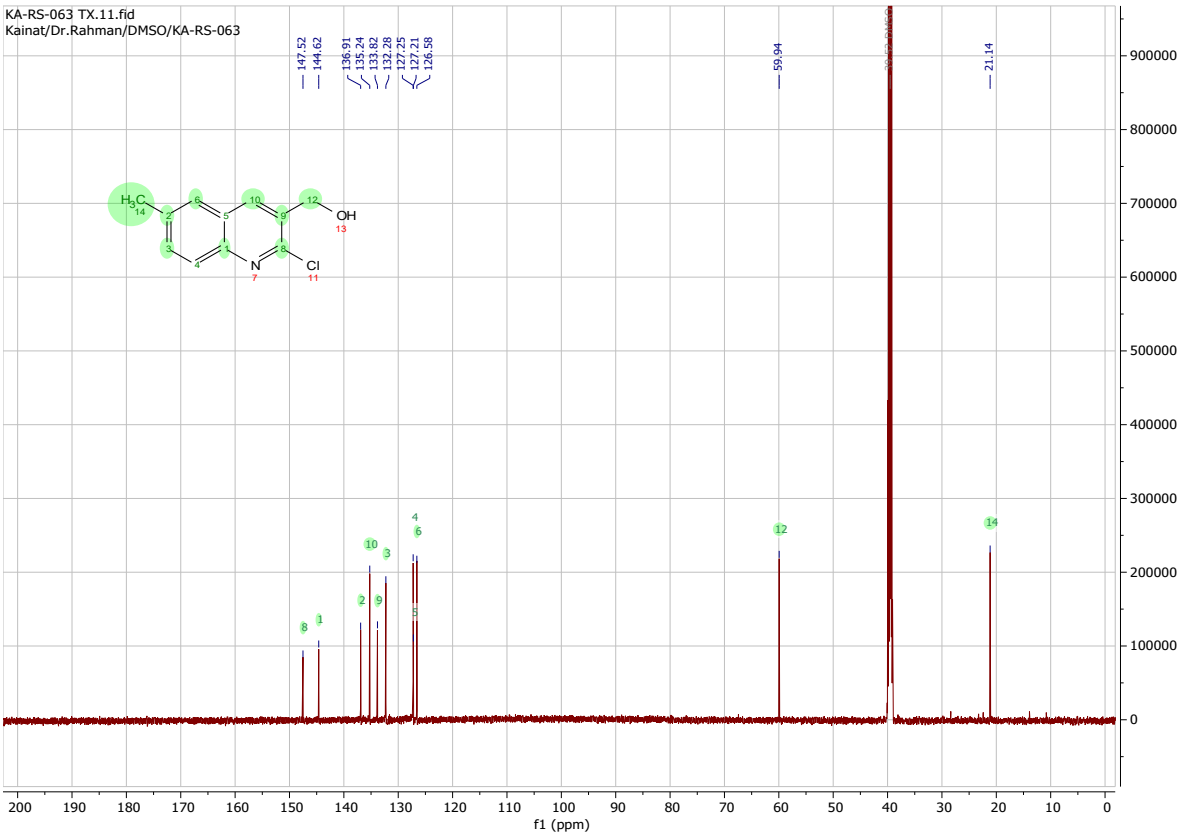

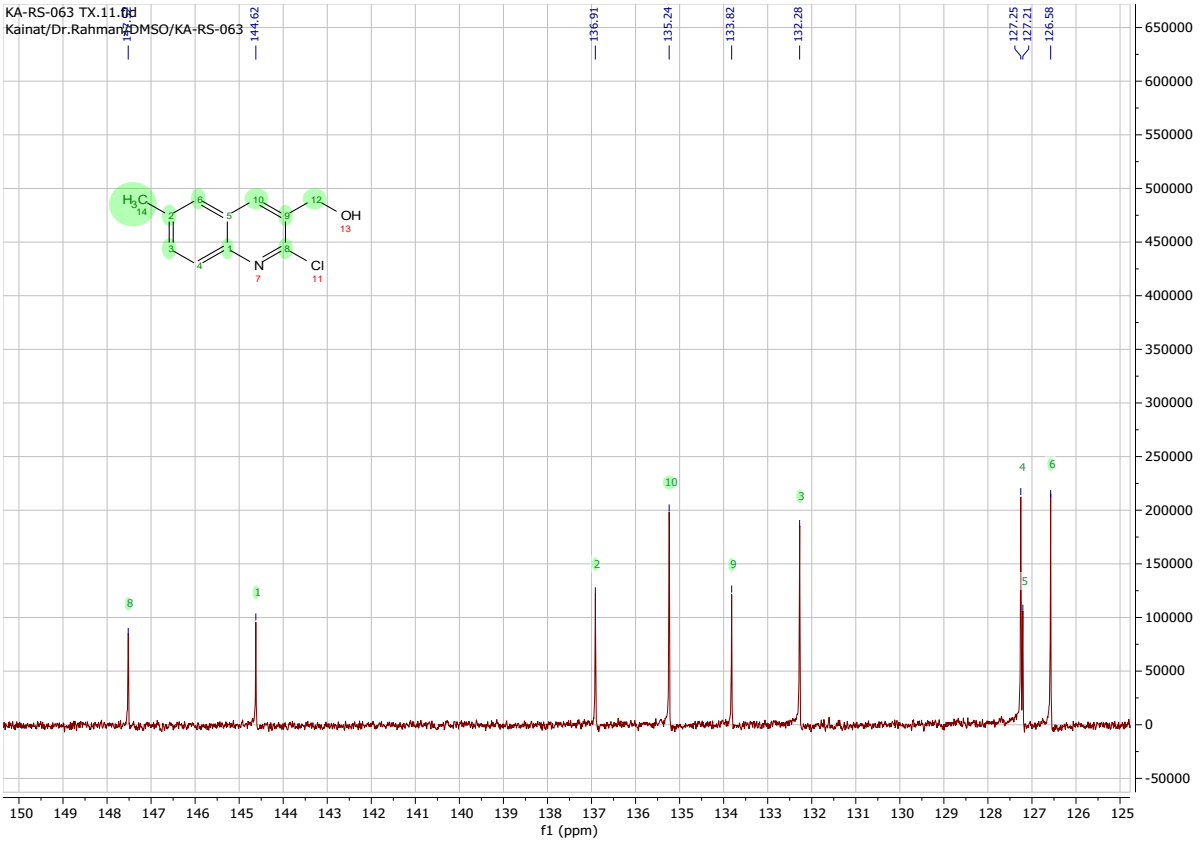
KA-RS-063 TX.11.10.1d
Kainat/Dr.Rahman/DMSO/KA-RS-063
144.62
136.91
135.24
133.82
132.28
127.25
127.21
126.58
OH
Cl
N
650000
600000
550000
500000
450000
400000
350000
300000
250000
200000
150000
100000
50000
0
-50000
150 149 148 147 146 145 144 143 142 141 140 139 138 137 136 135 134 133 132 131 130 129 128 127 126 125
f1 (ppm)

5.12 DEPT-135 NMR (DMSO, 150 MHz) of (2-Chloro-6-methylquinolin-3-yl)methanol) (2b)

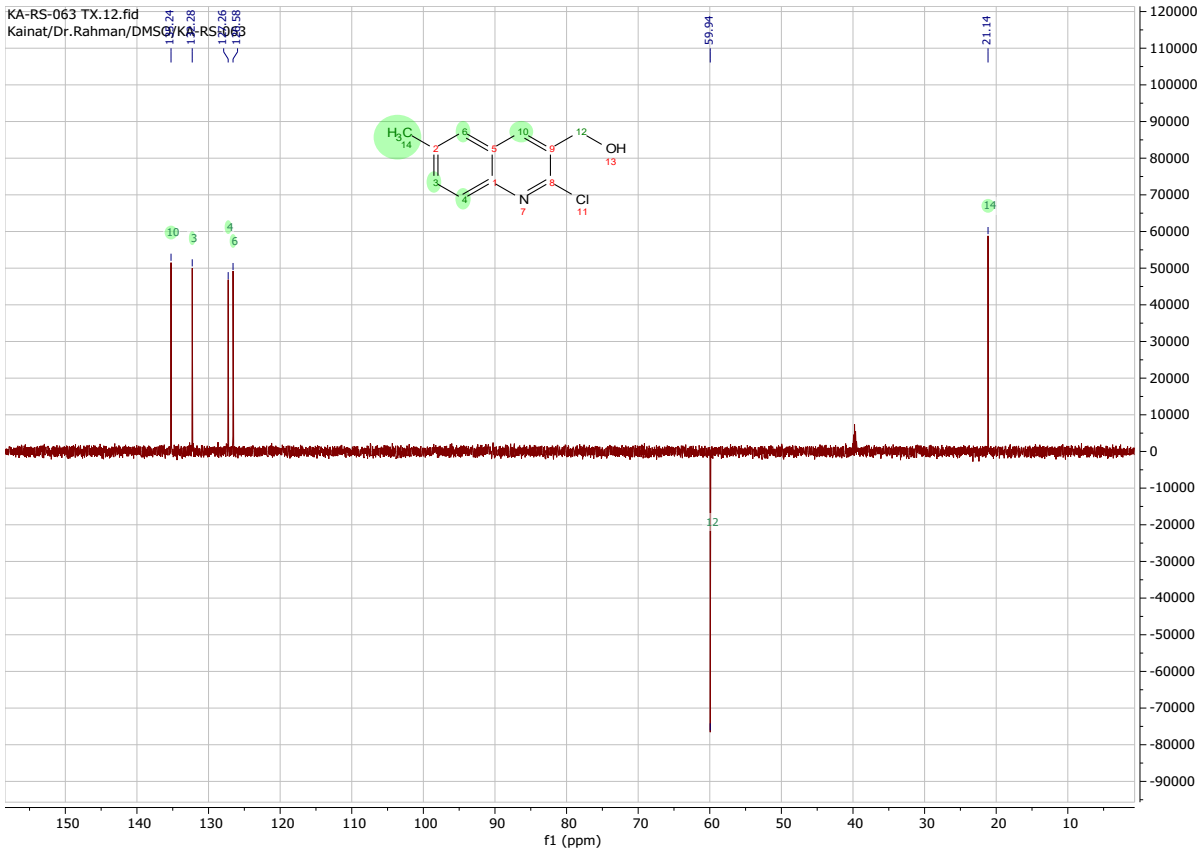

5.13 ^{1}H NMR ($CDCl_3$, 400 MHz) of (2-Chloroquinolin-3-yl)methyl 2-aminobenzoate (5a)

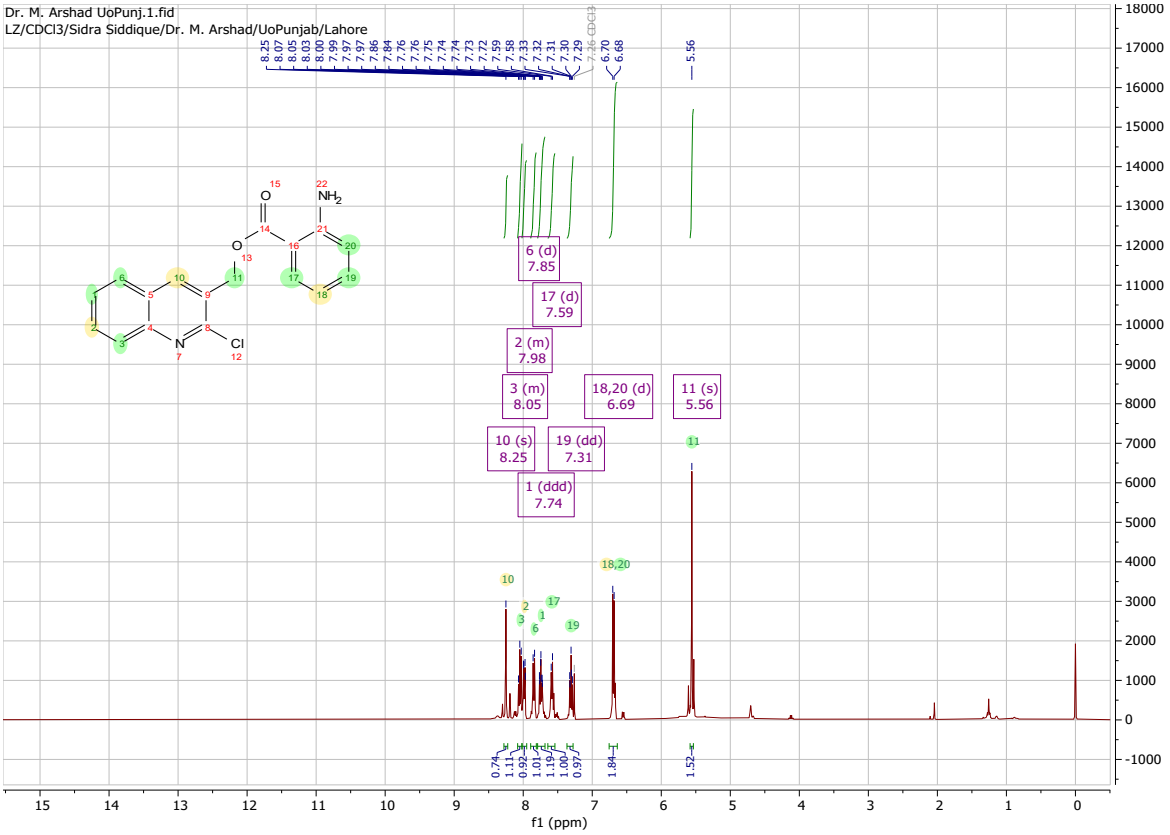

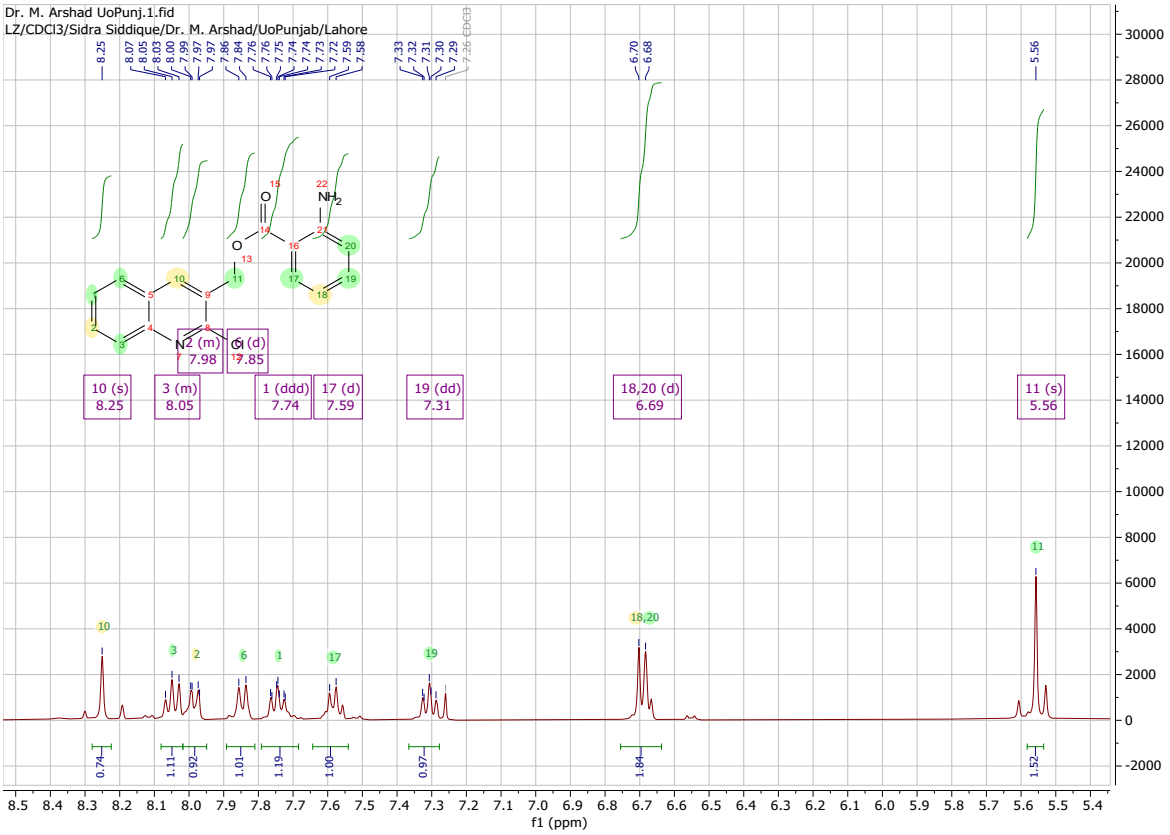

5.14 ^{13}C NMR ($CDCl_3$, 400 MHz) of (2-chloroquinolin-3-yl)methyl-2-aminobenzoate (5a)

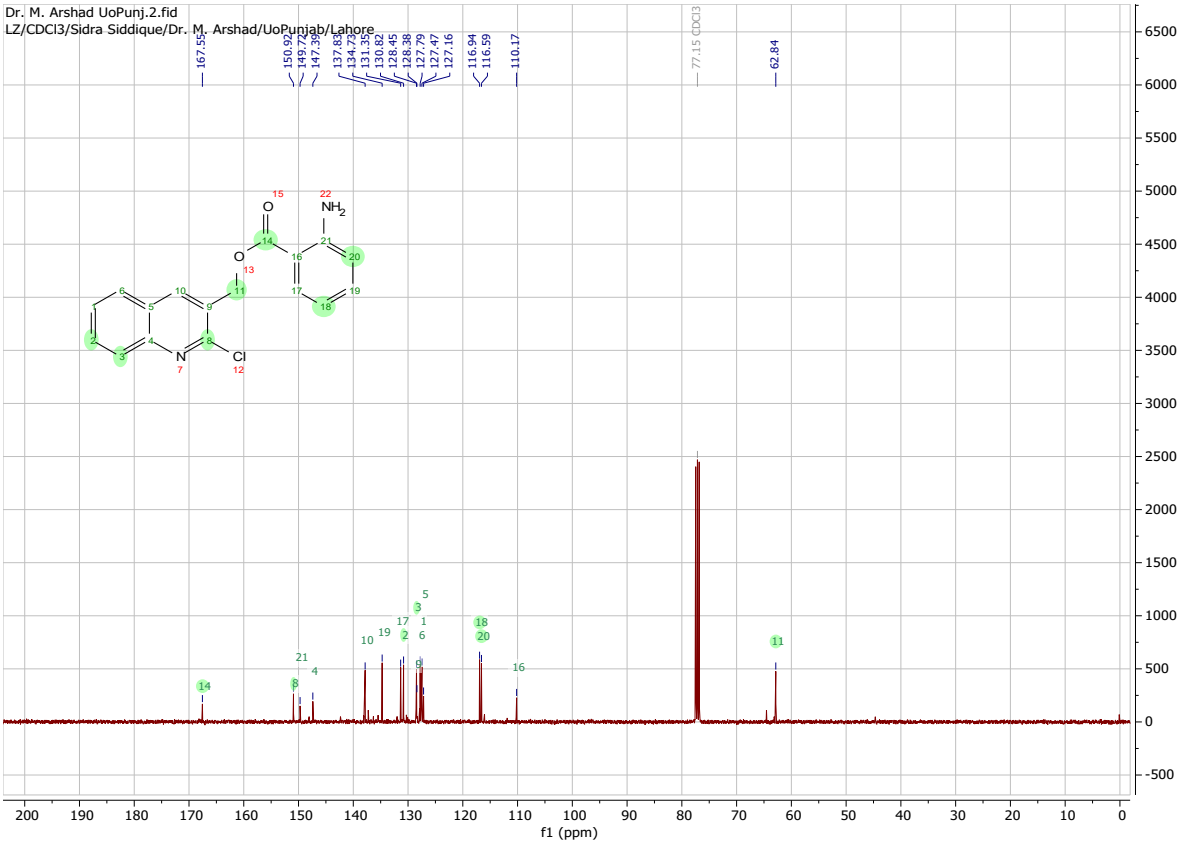

5.15 ^{1}H NMR ($CDCl_3$, 400 MHz) of (2-Chloro-6-methylquinolin-3-yl)methyl 2-aminobenzoate (5b)

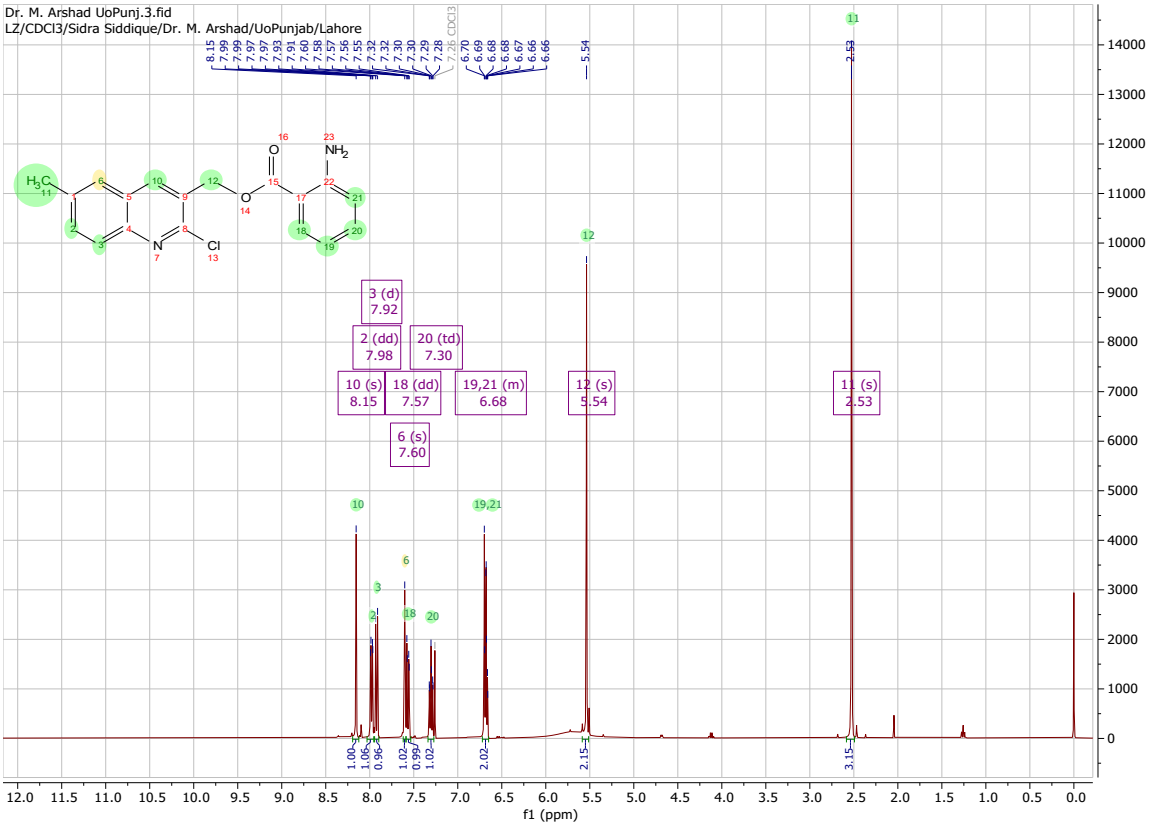

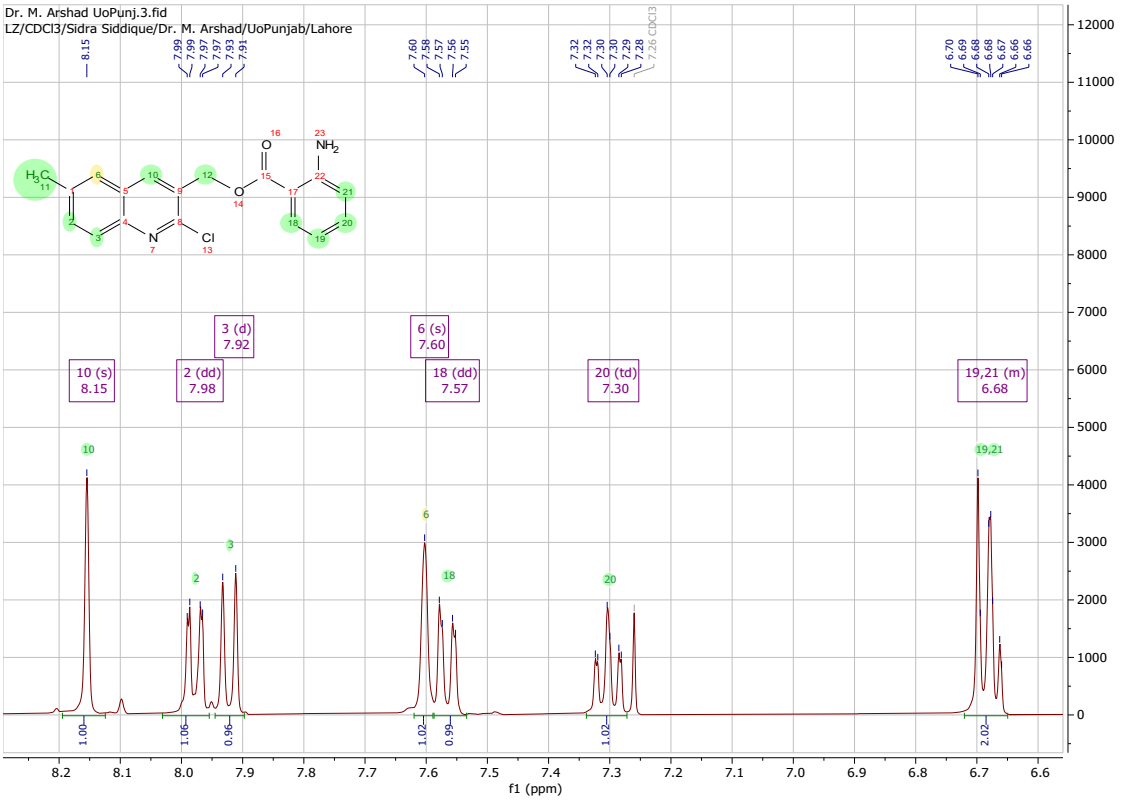

5.16 ^{13}C NMR ($CDCl_3$, 100 MHz) of (2-Chloro-6-methylquinolin-3-yl)methyl 2-aminobenzoate (5b)

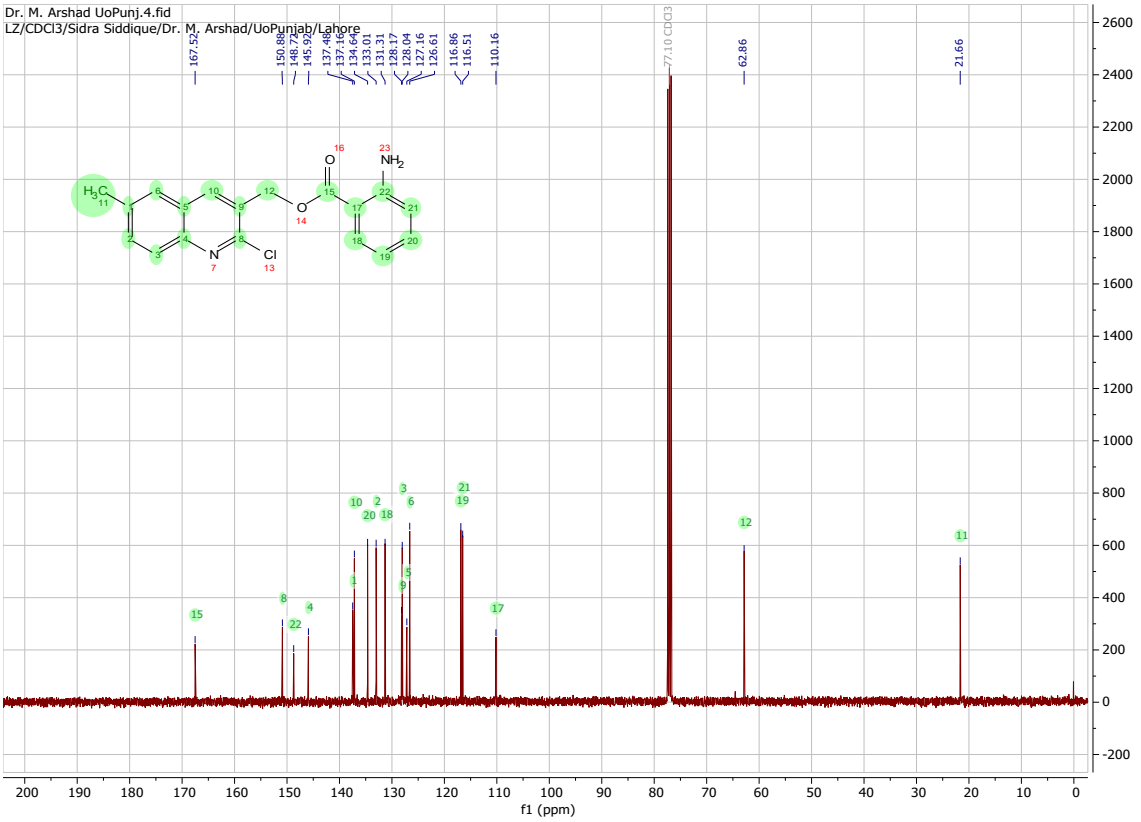

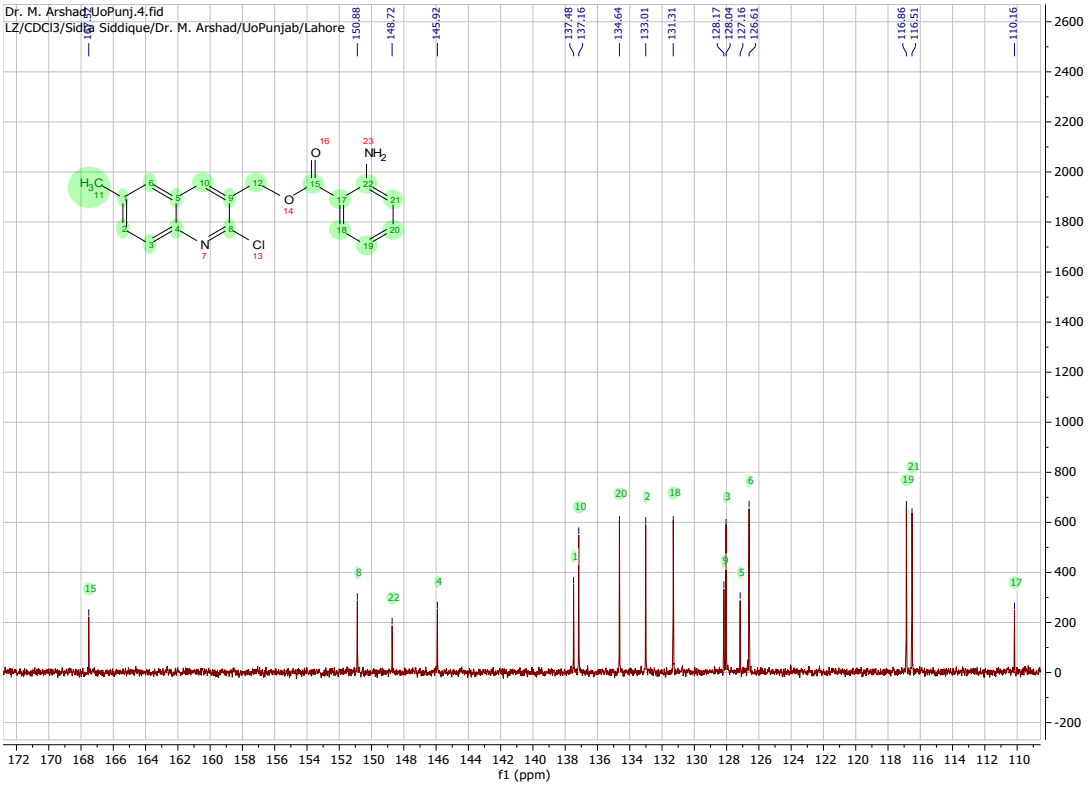

5.17 ^{1}H NMR (300 MHz, DMSO) of (2-Chloro-6-methoxyquinolin-3-yl)methyl-2-aminobenzoate (5c)

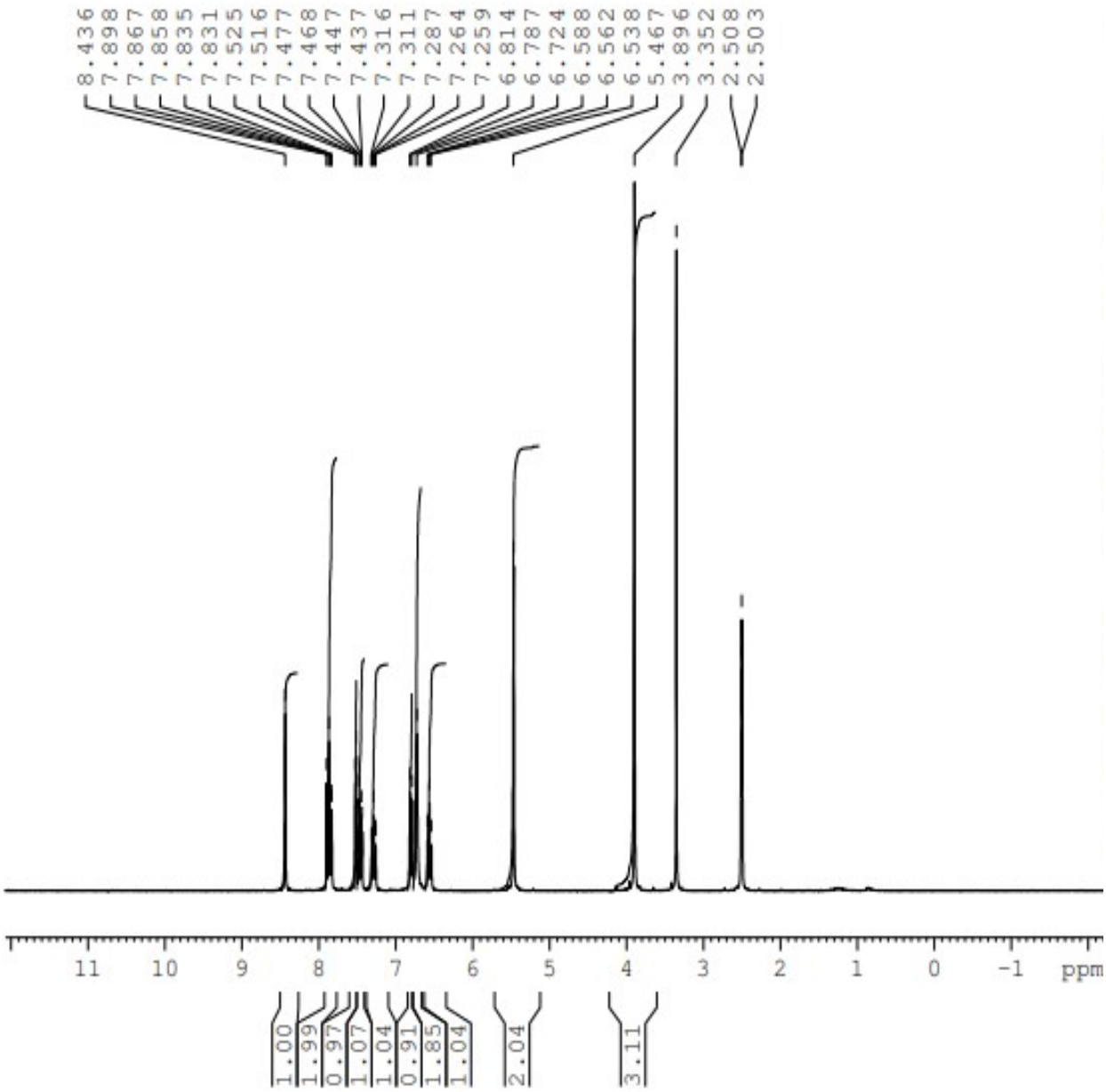

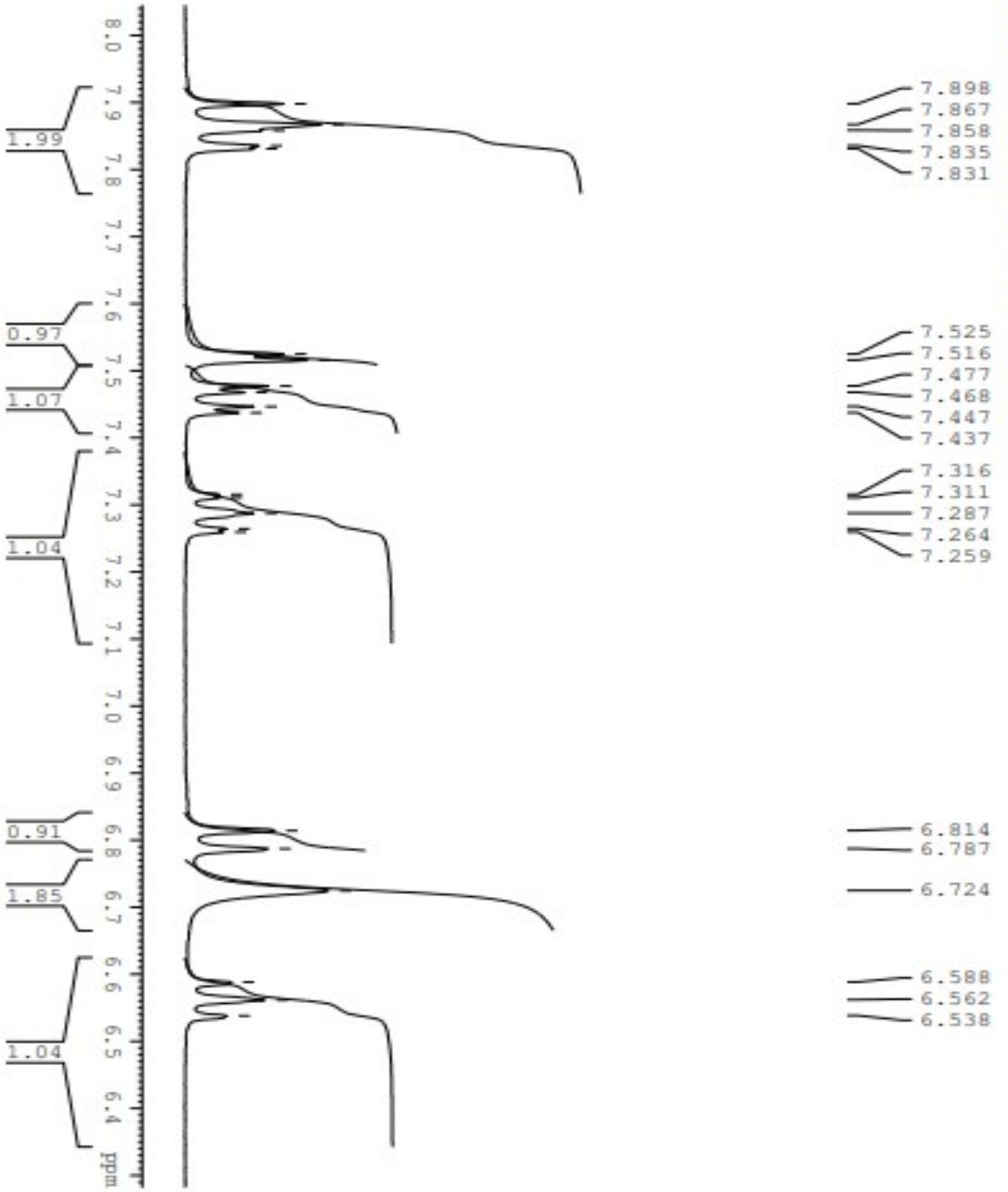
7.898
7.867
7.858
7.835
7.831
7.525
7.516
7.477
7.468
7.447
7.437
7.316
7.311
7.287
7.264
7.259
6.814
6.787
6.724
6.588
6.562
6.538
1.99
0.97
1.07
1.04
0.91
1.85
1.04
8.0
7.9
7.8
7.7
7.6
7.5
7.4
7.3
7.2
7.1
7.0
6.9
6.8
6.7
6.6
6.5
6.4
ppm

5.18 ^{13}C NMR (75 MHz, DMSO) of (2-chloro-6-methoxyquinolin-3-yl)methyl-2-aminobenzoate (5c)

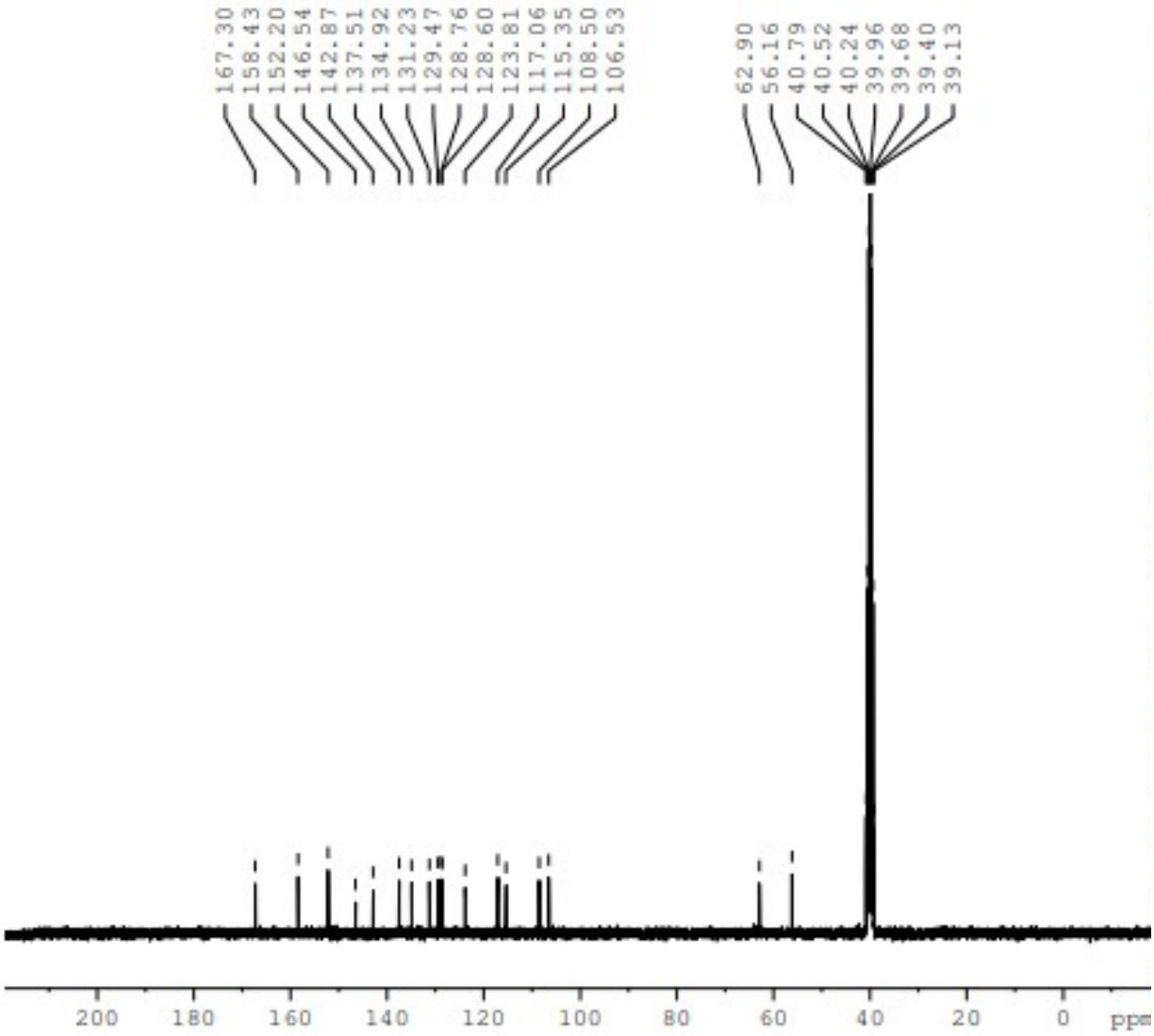

6 X-Ray Crystallography Data (XRD)

In quinoline ring the bond lengths of N1-C1 is 1.3094 (64) Å and of N1-C 5 is1.3678 (59) Å indicating the C=N and C-N bonds (Table S3 and S4).[4,5] The dihedral angle present between the amino benzoic acid and quinoline is 77.923 (13) Å. The root mean square deviations for the quinoline ring (C1/C2/C3/C4/C5/C6/C7/C8/C9/N1) system is 0.0129(41) Å, while the C18-atom of methyl group and Cl1 (chloro group) is away by 0.0456(92) Å and 0.0051(51) Å from the mean plane of fitted atoms of quinoline. The ester group (O1/O2/C10/C11) is deviating by 2.074(37) Å and 75.860(19) Å with the amino benzene and quinoline rings. The root mean square deviations for the aminobenzene ring (C12/C13/C14/C15/C16/C17) system is 0.0022(35) Å, while the C11-atom of methyl ester group and N2 (amino group) is away by 0.0500(51) Å and –0.0214(79) Å from the mean plane of fitted atoms of aminobenzene.

Table S3. Bond Lengths for compound **5b**

Atom	Atom	Length/Å	Atom	Atom	Length/Å
C1	N1	1.309(6)	C8	C18	1.514(7)
C1	C2	1.415(7)	C10	O2	1.449(6)
C1	Cl1	1.747(5)	C11	O1	1.213(5)
C2	C3	1.354(7)	C11	O2	1.354(5)
C2	C10	1.500(7)	C11	C12	1.461(6)
C3	C4	1.417(7)	C12	C13	1.398(6)
C4	C5	1.401(6)	C12	C17	1.417(6)
C4	C9	1.411(6)	C13	C14	1.367(7)
C5	N1	1.368(6)	C14	C15	1.371(7)
C5	C6	1.398(7)	C15	C16	1.369(8)
C6	C7	1.355(7)	C16	C17	1.393(7)
C7	C8	1.404(8)	C17	N2	1.354(6)
C8	C9	1.367(7)			

Table S4. Bond Angles for compound **5b**

Atom	Atom	Atom	Angle/°	Atom	Atom	Atom	Angle/°
N1	C1	C2	126.1(4)	C8	C9	C4	121.6(5)
N1	C1	Cl1	115.8(4)	O2	C10	C2	106.6(4)
C2	C1	Cl1	118.0(4)	O1	C11	O2	121.6(4)
C3	C2	C1	116.0(5)	O1	C11	C12	126.6(4)
C3	C2	C10	122.5(5)	O2	C11	C12	111.8(4)
C1	C2	C10	121.4(5)	C13	C12	C17	119.1(4)
C2	C3	C4	121.1(5)	C13	C12	C11	120.5(4)
C5	C4	C9	118.7(4)	C17	C12	C11	120.3(4)

Atom	Atom	Atom	Angle/°	Atom	Atom	Atom	Angle/°
C5	C4	C3	117.6(4)	C14	C13	C12	122.2(5)
C9	C4	C3	123.7(5)	C13	C14	C15	118.2(5)
N1	C5	C6	118.5(4)	C16	C15	C14	121.7(5)
N1	C5	C4	122.1(4)	C15	C16	C17	121.4(5)
C6	C5	C4	119.4(4)	N2	C17	C16	119.7(5)
C7	C6	C5	120.3(5)	N2	C17	C12	122.9(5)
C6	C7	C8	121.8(5)	C16	C17	C12	117.4(5)
C9	C8	C7	118.2(5)	C1	N1	C5	117.0(4)
C9	C8	C18	121.0(5)	C11	O2	C10	115.1(4)
C7	C8	C18	120.8(5)				

7 References

1. Kady IO. Microscale Electrophilic Aromatic Substitution of p-Toluidine. *J Chem Educ.* 1995; 72(1):A9. https://doi.org/10.1021/ed072pa9

2. Redasani VK, Kumawat VS, Kabra RP, Kansagara P, Surana SJ. Applications of green chemistry in organic synthesis. *Int. J. Chemtech Res.* 2010 Jul;2(3):1856-9.

3. Meth-Cohn O, Narine B, Tarnowski B. A versatile new synthesis of quinolines and related fused pyridines, Part 5. The synthesis of 2-chloroquinoline-3-carbaldehydes. *J. Chem. Soc., Perkin Trans. 1.* 1981:1520-1530. https://doi.org/10.1039/P19810001520

4. Khalid M, Arshad MN, Tahir MN, Asiri AM, Naseer MM, Ishaq M, Khan MU, Shafiq Z. An efficient synthesis, structural (SC-XRD) and spectroscopic (FTIR, 1HNMR, MS spectroscopic) characterization of novel benzofuran-based hydrazones: An experimental and theoretical studies. *J. Mol. Struct*. 2020;1216:128318. https://doi.org/10.1016/j.molstruc.2020.128318

5. Ahmed M, Qadir MA, Hameed A, Arshad MN, Asiri AM, Muddassar M. Azomethines, isoxazole, N-substituted pyrazoles and pyrimidine containing curcumin derivatives: Urease inhibition and molecular modeling studies. *Biochem. Biophys. Res. Commun.* 2017;490(2):434-440. https://doi.org/10.1016/j.bbrc.2017.06.059